Magnetic Resonance Spectroscopy

6

Sai Merugumala, Saadalah Ramadan, Walker Keenan, Huijun Liao, Luke Y-J. Wang, and Alexander Lin

Abbreviations

^{13}C	Carbon 13
2D COSY	Two-dimensional correlated spectroscopy
2D JPRESS	Two-dimensional J-resolved point-resolved spectroscopy
AD	Alzheimer's disease
BD	Bipolar disorder
CEST	Chemical exchange saturation transfer
Cho	Choline
Cr	Creatine
CRLB	Cramer–Rao lower bounds
CSI	Chemical shift imaging
FFT	Fast Fourier transform
FID	Free induction decay
fMRI	Functional magnetic resonance imaging
GABA	*Gamma*-aminobutyric acid
GABA-T	GABA transaminase
GAD	Glutamic acid decarboxylase
Gln	Glutamine
Glu	Glutamate
GluCEST	Glutamate chemical exchange saturation transfer
Glx	Both glutamate and glutamine
GPC	GlyceroPhosphoCholine
GPx	Glutathione peroxidase
GSH	Glutathione
GSSG	Glutathione disulfide
JPRESS	J-resolved point-resolved spectroscopy
LCModel	Linear compilation model
MCI	Mild cognitive impairment
MEGA-PRESS	Mescher–Garwood point-resolved spectroscopy
mI	Myoinositol
MRI	Magnetic resonance imaging
MRS	Magnetic resonance spectroscopy
NAA	*N*-Acetylaspartic acid
NAAG	*N*-Acetylaspartylglutamic acid
NMDA	*N*-Methyl-D-aspartic acid

S. Merugumala, MS • W. Keenan • H. Liao, BS
Department of Radiology, Brigham and Women's Hospital, Harvard Medical School, Boston, MA, USA

S. Ramadan, PhD
Faculty of Health, School of Health Sciences, University of Newcastle, Hunter Building, Callaghan, NSW 2308, Australia

L.Y.-J. Wang, MD
Department of Radiology, Brigham and Women's Hospital, Harvard Medical School, Boston, MA, USA

Department of Anesthesiology, Perioperative and Pain Medicine, Boston Children's Hospital, Harvard Medical School, Boston, MA, USA

A. Lin, PhD (✉)
Department of Radiology, Brigham and Women's Hospital, Harvard Medical School, Boston, MA, USA

Psychiatric Neuroimaging Laboratory, Brigham and Women's Hospital, Harvard Medical School, Boston, MA, USA
e-mail: aplin@partners.org

C. Mulert, M.E. Shenton (eds.), *MRI in Psychiatry*,
DOI 10.1007/978-3-642-54542-9_6, © Springer Berlin Heidelberg 2014

NMR	Nuclear magnetic resonance
PCP	Phencyclidine
PC	Phosphorylcholine
PCr	Phosphocreatine
PET	Positron emission tomography-PRESS, Point-resolved spectroscopy
ProFit	Prior knowledge fitting
RF	Radio frequency
ROI	Region of interest
ROS	Reactive oxygen species
STEAM	Stimulated echo acquisition mode
SVS	Single voxel spectroscopy
TCA	Tricarboxylic acid cycle
TE	Echo time
TI	Inversion time
TR	Relaxation time

6.1 Magnetic Resonance Spectroscopy: The Virtual Biopsy

6.1.1 Introduction

Research in neuroscience has slowly been trying to bridge the gap between understanding the difference between the brain and the mind. In this process, many of the concepts in cognitive psychology and psychiatry are being rewritten as development and application of new technologies further our understanding of the brain. The goal is to answer many of the questions that cognitive psychologists and psychiatrists have been seeking to understand. A particularly productive field of research has involved medical imaging that utilizes techniques such as functional magnetic resonance imaging (fMRI; as reviewed in this textbook (Posner and Raichle 1997)) or positron emission tomography (PET) (Friston 1997). Both techniques purport to measure neuronal activation; however, both only measure specific properties of the brain: blood flow in fMRI and glucose uptake with PET. The relationship between these measures and actual neuronal activity is a major assumption that is generally unquestioned. A growing number of scientists, psychiatrists, and philosophers are nonetheless beginning to question this assumption.

Until recently, there were no direct means to measure brain activity aside from animal studies in which neuronal activity was measured by electrodes implanted deep in the brain, clearly a very invasive technique (although electroencephalography as reviewed in this textbook can provide a related measure). A technique that could directly measure neuronal activity, could provide a noninvasive assay, and could explore brain systems as opposed to areas would be the ideal cognitive psychological tool: it exists as magnetic resonance spectroscopy (MRS), a noninvasive neurochemical assay that can directly measure neuronal activity, biochemical systems, and metabolic processes utilized by neurons.

6.1.2 Physics of MRS

A technique older than both fMRI and PET, nuclear magnetic resonance (NMR) spectroscopy, was first introduced in the early 1950s. Typically employed by the organic chemist to define chemical structures, NMR spectroscopy can in fact be applied to the human body, or more specifically to the human brain, providing quantitative and noninvasive studies of neurobiochemistry. The idea of using NMR to study the human body is by no means new. In fact, very soon after the first successful NMR experiments were conducted on test tube samples in 1946, Bloch, the pioneer of NMR, obtained a strong proton signal by placing his finger in the radio-frequency (RF) coil of his spectrometer (Andrew 1980). Although the potential of using NMR in biological systems was prevalent throughout the 1950s and early 1960s, it was not until the development of high-field superconducting magnets together with the emergence of fast Fourier transform (FFT) NMR did the potential of NMR in biological systems become realized (Ernst 1992). During this same time period, scientists began to realize that NMR machines could produce images of body structures that very quickly led to the advent of magnetic resonance imaging (MRI) as we know it today (Lauterbur 1989). This introduced whole body magnets with magnetic field strengths of 0.5–9.4 T, of which there are presently over 25,000 installed worldwide (Rinck 2012).

It was not until the late 1980s that industry standardization of spectroscopy occurred, heralding a new era of clinical applications of NMR, giving a new name (by dropping the word "nuclear"), magnetic resonance spectroscopy, or MRS, as well as a new lease to life to spectroscopy. The physics behind the technique is fundamentally the same as that utilized by early NMR: the sample (patient) slides into the bore of the magnetic where there is a uniform static magnetic field such that unbound nuclei are oriented parallel and antiparallel according to their spin state. A radio-frequency (RF) coil is then placed near the body part of the patient to maximize the amount of signal that can be obtained. The nuclei are then excited by electromagnetic radiation in the form of a pulse sequence via a transmitter. The nuclei absorb the energy, altering the nuclear spin. As the nuclei precess or "relax" back to their original state, energy is released and detected by the receiver in the RF coil as a free induction decay, which is promptly fast Fourier transformed into the resulting spectra (Fig. 6.1).

Each chemical resonates at established frequencies that upon Fourier transform results in peaks at specific locations, or chemical shifts, along the *x*-axis. The chemical shift of each chemical is governed by the structure of the chemical, in particular, the grouping of the hydrogen atoms as single or multiple peaks (singlets and multiplets), and proximity to other hydrogen-containing groups (*J*-coupling). These chemical shifts are often expressed as "parts per million," which can be confusing as it does not relate to the concentration of the chemical, but historically has been used to express the frequency. The use of this nomenclature is so that it is not dependent upon the field strength of the magnet used such that the resonance frequencies are the same between a 1.5 T MRI scanner and a 3.0 T scanner. The concentration of the metabolite is expressed along the *y*-axis as the height of the peak such that higher concentrations result in higher peaks and vice versa. Quantitation of these peak heights can provide an objective measure of brain biochemistry that is similar to a blood test

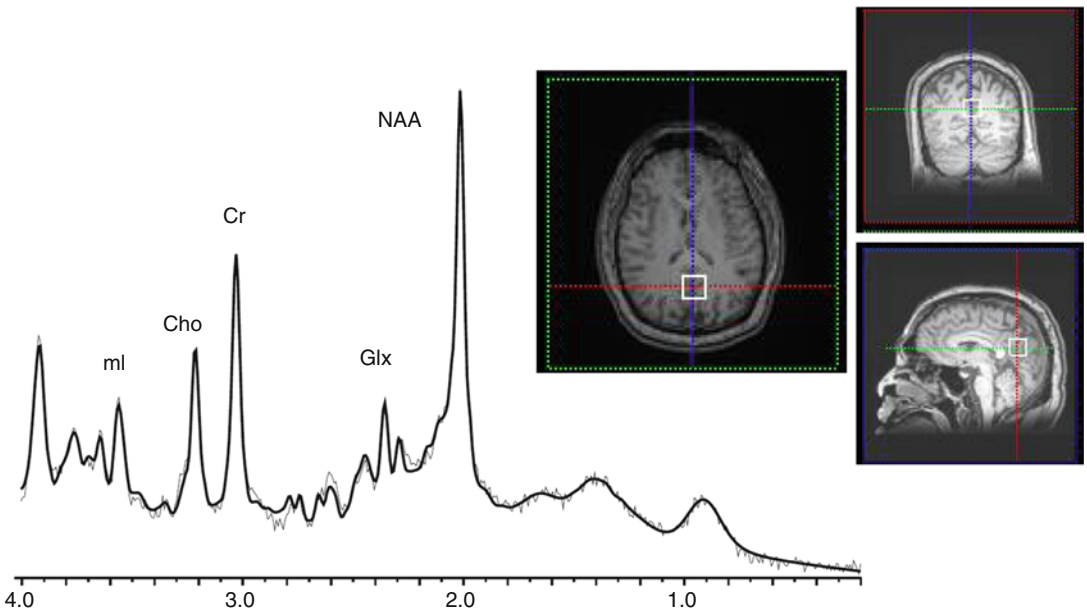

Fig. 6.1 Representative proton spectrum acquired from the posterior cingulate gyrus. Data were acquired using a 3 T clinical MRI scanner and point-resolved spectroscopy localization with an echo time of 30 ms and repetition time of 2 s. Voxel location is shown in the *inset* to the right in the axial, coronal, and sagittal planes. Major metabolites of *N*-acetylaspartate (*NAA*), glutamate and glutamine (*Glx*), creatine (*Cr*), choline (*Cho*), and myoinositol (*mI*) are labeled

or lab analysis: different concentrations are measured and reported, which can then be used for diagnosis or disease characterization. More importantly, however, the role of each of the chemicals is tied to metabolic and physiological processes within the brain that directly relate to cognitive or neuronal processes. The remainder of this chapter will be devoted to the major metabolites that are detected by MRS, as well as the different methods by which the data can be collected.

6.2 *N*-Acetylaspartate (NAA): Neuronal Marker

As indicated in the spectra in Fig. 6.1, one of the chemicals that can be measured by MRS is NAA. The primary resonance of NAA is at 2.02 ppm. It is an amino acid derivative synthesized in neurons and transported down axons. It is therefore a putative "marker" of viable neurons, axons, and dendrites. Studies where NAA was labeled with fluorescent tags demonstrated that NAA was distributed throughout the neuron and axon (Moffett et al. 1993). Studies have also correlated the concentration of NAA in the brain with the number of neurons measured (Urenjak et al. 1992). The ability to quantifiably measure neuron populations allows MRS to provide a diagnostic tool that no other radiological technique can match: an ability to literally "count" the number of active brain cells using a completely noninvasive and quantitative technique by simply measuring the peak height of the NAA chemical in the MRS spectra. This can be utilized in a number of practical means. For example, every metabolite has a "normal" concentration that generates a pattern of peaks that is the same from person to person unless there is an underlying pathology. Diagnosis with MRS can therefore be made either by comparing the numeric values of metabolite concentrations or by recognizing abnormal patterns of peaks in the spectra. With either method, it is the increase or decrease in the concentrations of the metabolites that is diagnostic for pathology as has been shown across a broad variety of diseases (Lin et al. 2005; Harris et al. 2006; Moffett et al. 2007). However, it should also be noted that NAA is a cerebral metabolite that participates in a number of metabolic processes, and therefore, the interpretation of NAA as solely a neuronal marker is somewhat of an oversimplification (Barker 2001). It is important to understand the context of NAA metabolism, as detailed below.

6.2.1 NAA Metabolism

NAA is formed by the transamination of glutamate (Glu)with oxaloacetate which leads to aspartate (Asp) (Cooper et al. 1970), and in the presence of acetyl coenzyme A and NAA synthase, (L-aspartate *N*-acetyltransferase), aspartate (Asp) is converted to NAA. This process occurs primarily, but not exclusively, in neurons, where it exhibits a very high intracellular–extracellular gradient. NAA is hydrolyzed back into aspartate and acetate by aspartoacylase (*N*-acetyl-L-ASPARTATE amidohydrolase) in mature oligodendrocytes only. In some neurons, a portion of NAA is turned into *N*-acetylaspartylglutamate (NAAG) in the presence of glutamate (Glu) by an NAAG synthase (*N*-acetylaspartate-L-glutamate ligase) (Baslow 2000). NAA and NAAG are major neuronal osmolytes, and the large amount of NAA and NAAG present in the brain can serve as cellular reservoirs for Asp and Glu. Since both are polar and ionizable hydrophilic molecules that undergo a regulated efflux into extracellular fluid, they can also play a role in water movement out of neurons (Baslow 2000). In addition, the fact that the NAA-metabolizing enzyme aspartoacylase is an integral component of the myelin sheath suggests that intraneuronal NAA may supply the acetyl groups for myelin lipid synthesis (Chakraborty et al. 2001). Finally, the cell type-specific metabolic enzymes in the NAA and NAAG cycle indicate a three-cell compartmentalization involving neurons, astrocytes, and oligodendrocytes. Those neurons that may synthesize NAAG from NAA and Glu target the release of NAAG to astrocytes,

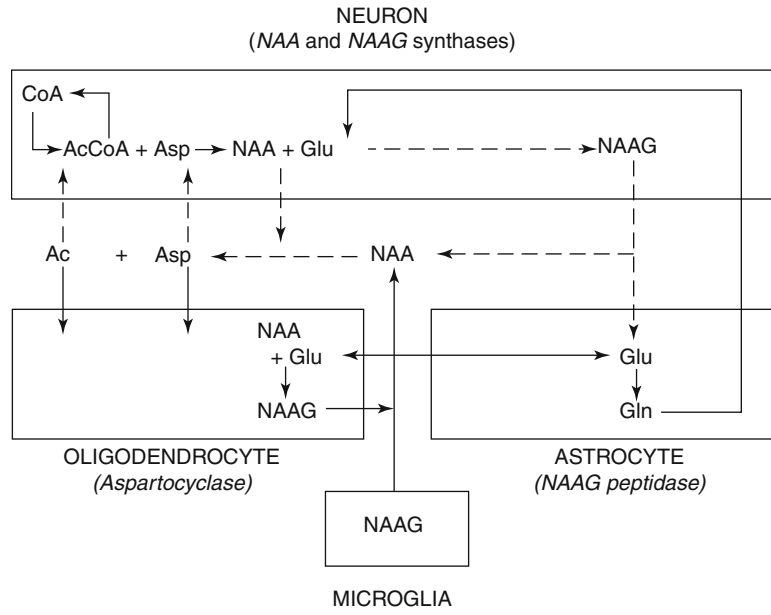

Fig. 6.2 Tricellular NAA–NAAG cycle operating between neurons, astrocytes, and oligodendrocytes (Modified from Baslow 2010). *CoA* coenzyme A, *Acetyl-CoA* acetyl coenzyme A, *Asp* aspartate, *Glu* glutamate, *Gln* glutamine, *NAA N*-Acetylaspartate, *NAAG* *N*-Acetylaspartylglutamate

where it is cleaved into NAA and Glu. The Glu is taken up by astrocytes, where it may be returned to neurons via the glutamate–glutamine cycle. The residual NAA extracellular products are removed and hydrolyzed by oligodendrocytes (Baslow 2000). This unique tricellular metabolic cycle, as shown in Fig. 6.2, involving NAA and NAAG, provides a potential glial cell-specific signaling pathway, which can also be reflected in changes in different diseases (Baslow 2010).

6.2.2 Measuring NAA Using Single Voxel Spectroscopy

As a "virtual biopsy," localization is required when examining specific regions of the brain involved in disease. Localization is defined by a region of interest, or voxel, from which the spectrum is acquired and, hence, described as single voxel spectroscopy (SVS). This region is a cube within the brain that can be visualized and placed in the sagittal, coronal, and axial planes as shown in Fig. 6.1. The localization is achieved by utilizing a pulse sequence that acquires the MRS signal. Though several sequences, and permutations of sequences, exist which are capable of yielding an in vivo MRS spectra, many of them are research techniques and not widely available (although discussed later in this chapter). The two most commonly used sequences are PRESS and STEAM as described below:

6.2.2.1 Point-Resolved Spectroscopy (PRESS)

The point-resolved spectroscopy (PRESS) sequence is a standard part of the software package that accompanies the two most popular MRI manufacturers, Siemens (Erlangen, Germany) and General Electric (Waukesha, Wisconsin). On Siemens scanners, it is known as "svs_se." On General Electric machines, the sequence is called "Probe-P." The PRESS sequence was originally developed in 1987 by Paul Bottomley at General Electric (Bottomley 1987) and utilizes three orthogonal magnetic field gradients along the x-, y-, and z-axes using slice-selective 90° pulse followed by two slice-selective 180° pulses to select a specific three-dimensional voxel, within which a proton MRS spectrum can be obtained.

6.2.2.2 Stimulated Echo Acquisition Mode (STEAM)

STEAM also uses a series of three consecutive slice-selective 90° pulses for localization. However, the sequence only yields half as much detectable magnetization; therefore, the signal-to-noise ratio is halved. Nonetheless, adequate water suppression—which is necessary for all MRS techniques, as the metabolites to be detected exist at much lower concentrations than water—is more easily accomplished via STEAM (Haase et al. 1986). Shorter echo times are also attainable with STEAM, which may provide an advantage when detecting short T2 metabolites such as γ-aminobutyric acid (GABA).

6.2.2.3 Post-processing Single Voxel Data

SVS data can be post-processed and analyzed in several different ways. All major MR platforms have their own methods of reconstructing the data where the details are somewhat different, but the end result is generally an automated or semiautomated fitting of the metabolite peaks and a quantitative measure of major metabolites (NAA, creatine, choline, myoinositol), usually as a ratio to creatine to provide a normalization factor to account for differences in the peak area or amplitude between subjects which will differ depending on parameters such as the voxel size, number of averages, transmit gain, etc. The MRS data can also be exported for further analysis using MRS post-processing packages such as LCModel (Provencher 1993), jMRUI/AMARES (Vanhamme et al. 1997), etc. The advantage of this more sophisticated post-processing is that it allows for "absolute quantitation" of the metabolites by incorporating prior knowledge or additional measures (Kreis et al. 1993) that provide a concentration in millimolar per kilogram wet weight that would be equivalent to in vitro measurements of metabolite concentrations. While the accuracy of the quantitation, in terms of "absolute" quantitation, is somewhat controversial, the advantage of this method is that the metabolites can be quantified without being a ratio to creatine. This is especially important in diseases that can cause a change in creatine, in which case it is unclear whether it is the major metabolite that has altered or creatine or both.

6.2.3 Measuring NAA Using Chemical Shift Imaging (CSI)

One of the drawbacks of SVS is the natural limits of a single area of acquisition. Obtaining spectra in many different areas of the lesion would be time consuming. Multivoxel spectroscopy, also called chemical shift imaging (CSI) or spectroscopic imaging, overcomes this issue by adding an additional phase-encoding step that allows for spatial encoding of a larger volume such that it is divided into smaller voxels that can be summed or selected chemical shifts can be color-coded into chemical shift maps. In experimental duration, some two to three times longer than that in which a single voxel method acquires the spectrum of a single ROI, the CSI technique (Maudsley et al. 1983) can collect an array of spectra from a single plane.

6.2.3.1 CSI Pulse Sequence

STEAM and PRESS are still utilized for localization; however, phase-encoding gradients are employed to encode the spatial dimensions, and the MR signal is collected in the absence of any gradient in order to maintain the spectroscopic information. Each acquired ROI contains an MR spectrum that allows for the assessment of the metabolic profile of a specific location or allows for visualization of the spatial distribution of specific metabolites of interest. CSI also allows for the acquisition of smaller volumes than in single voxel techniques (as small as 0.4 cm^3 at higher magnetic field strength). This has the advantage over single voxel MRS techniques, as multiple brain regions can be assessed using the CSI technique which can also be completed offline via post-processing routines that allow for positioning of different areas of interest, assuming that they are contained with the larger region of interest selected for CSI acquisitions. Furthermore, there are additional variants of CSI that utilize different phase-encoding methods to either reduce scan time or allow for additional spatial

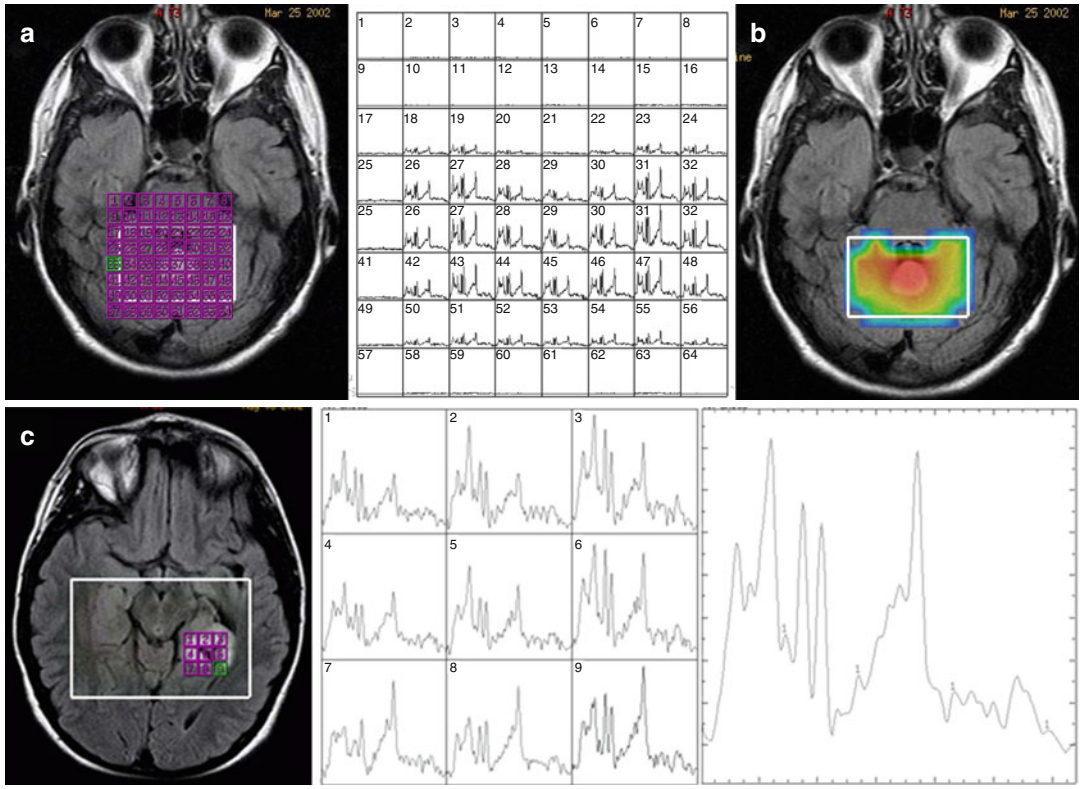

Fig. 6.3 Representative chemical shift imaging. (**a**) *Left*: MRI image with grid of voxels indicated in purple. *Right*: reconstruction of CSI data as individual spectra. (**b**) Metabolite map of NAA. (**c**) Simplified display of CSI data as a small grid of spectra as indicated on the image (*left*) and individual spectra (*middle*) and summed spectra (*right*)

resolution and information such as spiral phase encoding, echo planar sequences, multislice sequences, and parallel imaging methods (Posse et al. 2013).

6.2.3.2 Reconstruction of CSI Data

The main advantage of CSI is that the spatial information is retained such that during post-processing one can characterize the spectra in a number of different methods. The field of view can be partitioned into individual voxels determined by the resolution of the phase encoding. For example, if 16 frequency encodes and 16 phase encodes are used in a 16-cm^2 field of view and 1-cm slice thickness, each voxel will have a resolution of $1 \times 1 \times 1$ cm^3, and a spectrum can be reconstructed in each voxel as shown in Fig. 6.3a. Analyzing each voxel would be time consuming, and therefore, there are two different ways to display the data. First, one can create a "metabolite map" which selects a certain region of the spectrum, for example, 2.0–2.05 ppm for NAA, which creates a map based on the signal intensity of the spectrum from that spectral region, which is then displayed on top of the MRI image as shown in Fig. 6.3b. The spatial resolution of the metabolite maps are often interpolated which may result in over-interpretation of the true voxel resolution. There are also issues with signal correction where some areas may appear to have increased SNR but overall signal may be increased in that region, leading to possible misinterpretation of the data. It is therefore somewhat dangerous to rely solely on metabolite maps without evaluating the individual spectra. One can sum all of the spectra from a certain region of the spectrum, much like a single voxel acquisition as shown in Fig. 6.3c. This procedure is repeated at multiple regions in the CSI volume. The major advantage of CSI is that in post-processing, the ROI can be readily shifted to any location with the excitation volume.

However, CSI suffers from the disadvantage that the shape of individual ROIs is less well defined than in single voxel techniques. This can result in the adjacent ROIs being contaminated by large-amplitude signals from surrounding ROIs. Furthermore, CSI is not as reproducible as SVS (Rosen and Lenkinski 2007) and therefore is less sensitive to the more subtle changes. Finally, on most clinical scanners, the majority of CSI acquisitions are set up for long echo MRS which also eliminates important diagnostic metabolites such as glutamate Glu or myoinositol (mI), although for NAA, the focus of this section, it is sufficient.

6.2.4 Whole-Brain NAA

As described above, single voxel and CSI methods suffer from issues such as lipid contamination, voxel registration, as well as assumptions of T1 and T2 relaxation times. One method of addressing the aforementioned issues is to take advantage of the fact that NAA is the most prominent peak within the MRS spectrum (thus having a high signal-to-noise ratio) that acquires signal from the entire head and is thus named whole-brain NAA (WBNAA) spectroscopy (Rigotti et al. 2007). Unlike the single voxel and CSI methods, WBNAA does not utilize localization and instead acquires data immediately after excitation (TE = 0 ms) with a very long repetition time (TR = 10 s) and a short inversion time (TI = 940 ms). The inversion pulse is alternated between each acquisition where the TI is designed to null the NAA signal. The even and odd acquisitions are then subtracted from one another which nulls those metabolites, including lipid, that have a short T1 relaxation time. As NAA has a long T1 relaxation time (1.4 s), it remains visible. As a result of the long TR, there are no T1- or T2-weighting effects. The WBNAA signal is then normalized to the total brain volume as can be obtained from brain segmentation. This method operates under the assumption that all NAA arises from within the brain, and given the lack of localization, results of such studies would imply global effects of the disease.

6.2.5 NAA in Psychiatric Diseases

6.2.5.1 Schizophrenia

A recent meta-review of spectroscopy papers in schizophrenia revealed 103 papers alone that focused on MRS which included a total of 2,067 subjects and 2,115 controls of which the great majority of the studies focused on treated chronically ill patients (Kraguljac et al. 2012). All papers utilized either the SVS or the CSI methods, thereby allowing for regionalized differences to be measured. Decreased levels of NAA were found all across the brain including structures such as the hippocampus, thalamus, and frontal and temporal lobes. While the temporal lobes showed the greatest decreases in NAA with a standardized mean difference of −0.72, the variability of measurements in the temporal lobe were also greater than any other area of the brain. The reason for this variability is due to the susceptibility artifacts that occur due to the air and bone tissue interfaces within this brain region that result in distortions and signal loss (Olman et al. 2009). The basal ganglia and frontal lobe showed the most consistent decreases in NAA. While WBNAA measures have not been applied to schizophrenia, these global changes in NAA throughout the schizophrenic brain would indicate that this method would be sensitive to these changes.

6.2.5.2 Dementia

Given the relationship between NAA and neuronal viability, NAA is a key biomarker for dementia. Dozens of papers have shown decreases in NAA in both cortical and white matter regions of the brain including the posterior cingulate gyrus, the temporal lobe, and the occipital lobe (Graff-Radford and Kantarci 2013). In combination with myoinositol (mI), a putative glial marker, NAA provides up to 90 % sensitivity and 95 % specificity for distinguishing Alzheimer's disease (AD) from healthy subjects (Kantarci 2007). In a recent study, the ratio of NAA/mI predicted progression to mild cognitive impairment (MCI) or dementia in 214 subjects (Kantarci et al. 2013), which

supports previous findings of reduced NAA in MCI patients. Furthermore, MRS is valuable in differentiating between different types of dementia such as the Lewy body, frontal lobe, and vascular dementia (Shonk et al. 1995; Kantarci et al. 2004). While the temporal lobe is often thought to be the ideal location for detecting Alzheimer's disease, it is the posterior cingulate gyrus that has been shown to be the most sensitive to AD. While there may be a neuropathological role for the posterior cingulate cortex in AD, as has been shown in PET studies (Minoshima et al. 1997), this region of the brain is also one of the most homogeneous parts of the brain that results in spectra of superior technical quality, which would also contribute to the diagnostic sensitivity of MRS to AD and other dementias.

6.2.5.3 Depression/Bipolar Disorder

Changes in NAA in bipolar disorder and major depression have also been studied extensively (Capizzano et al. 2007). Several studies have shown reductions in NAA/Cr in the temporal lobes as a result of bipolar disorder. Some studies have also shown reductions in NAA/Cr in the frontal lobe in patients suffering from major depression; however, there are also studies that were not able to replicate these results. This may be due to the fact that a majority of the studies used a ratio to Cr despite the fact that some studies have shown that Cr is altered as a result of major depression (Gruber et al. 2003).

6.3 Glutamate: Excitatory Neurotransmitter

Glutamate (Glu) is an amino acid with several important roles in the brain. First, it is the most abundant excitatory neurotransmitter in the human brain, where it plays a major role in neurotransmission and where it is released from presynaptic cells and then binds to postsynaptic receptors, thus inducing activation as shown in Fig. 6.4. As a result, many neurological and psychiatric diseases have an impact upon Glu. In particular, dysfunction reflected in excessive Glu release or reduced uptake can lead to an accumulation of Glu, which results in excitotoxicity. This second mechanism is key to not only understanding the underlying pathophysiology of different brain disorders but also providing a potential pathway for disease treatment. The existence of numerous Glu agonists and antagonists now allows for pharmaceutical interventions that can be used to modulate glutamate Glu levels and thus provide potential treatments. Finally, Glu is a key compound in brain metabolism via the citric acid cycle and therefore also tightly coupled to brain energetics.

6.3.1 Glutamate and Glutamine Metabolism

Metabolically, glutamate (Glu) is stored as glutamine (Gln) in the glia, and the balanced cycling between these two neurochemicals is essential for normal functioning of brain cells. Glu and Gln are compartmentalized in neurons and glia, respectively, and this chemical interconversion reflects an important aspect of metabolic interaction between these two types of cells. In vivo studies have revealed that the neuronal/glial Glu/Gln cycle is highly dynamic in the human brain and is the major pathway of both neuronal Glu repletion and astroglial Gln synthesis (Gruetter et al. 1994; Mason et al. 1995). After its release into the synaptic cleft, Glu is taken up by adjoining cells through excitatory amino acid transporters. Astrocytes are responsible for the uptake of most extracellular Glu via Glu transporters and additionally have a vital role in preserving the low extracellular concentration of Glu needed for proper receptor-mediated functions, as well as to prevent excitotoxicity (Schousboe 2003; Schousboe and Waagepetersen 2005). Once taken up into the astrocyte, Glu is rapidly converted to Gln by the enzyme Gln synthetase. Small quantities of Gln are also produced de novo or from GABA (Hertz and Zielke 2004; Bak et al. 2006). Gln is released from astrocytes, accrued by neurons, and converted to Glu by the neuron-specific

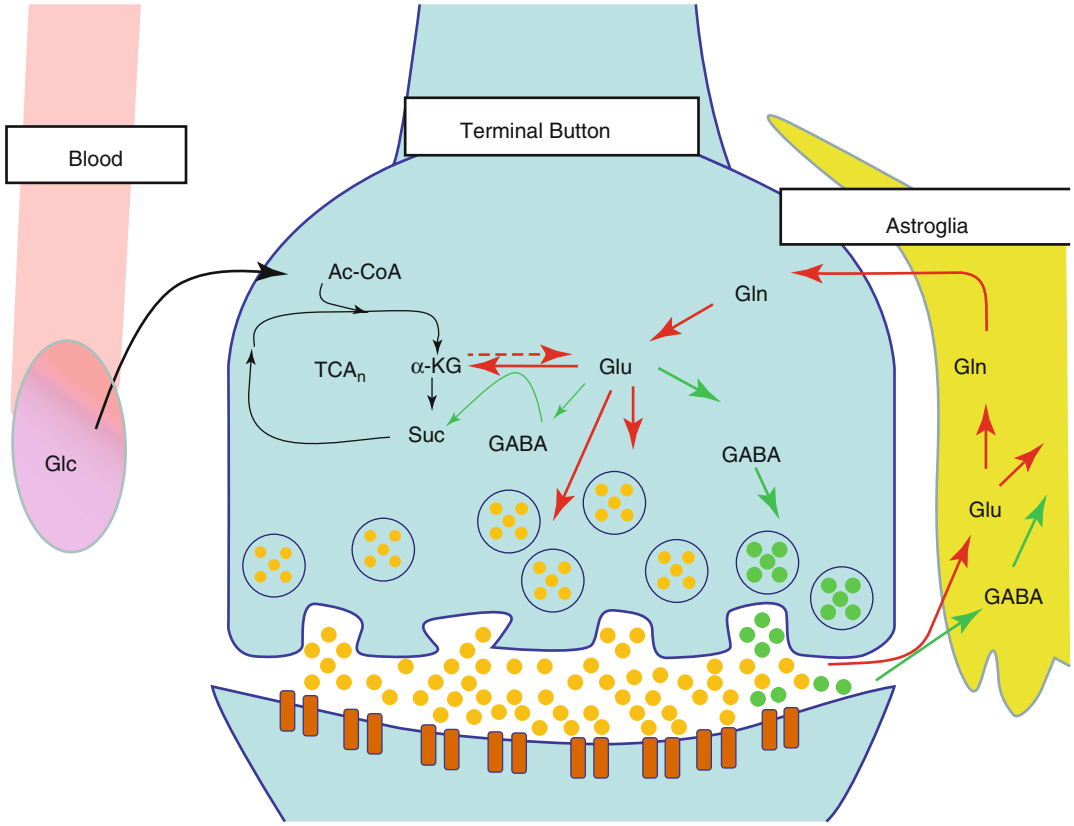

Fig. 6.4 Glutamate cycle in the neuron and glia. Glucose (*Glc*) from the capillaries is the primary source of fuel for the neurons which are then metabolized via the tricarboxylic acid cycle (*TCA*) to acetyl coenzyme A (*acetyl-CoA*), then to alpha-ketoglutarate (*α-KG*), and finally to succinate (*Suc*). α-KG is transaminated to glutamate (*Glu*), which can be further metabolized to gamma-aminobutyric acid (*GABA*). However, it is primarily released by the neuron and then taken up into the astroglia and metabolized to glutamine (*Gln*)

enzyme phosphate-activated glutaminase (Bak et al. 2006). Gln is the main precursor for neuronal Glu and GABA (Hertz and Zielke 2004), but Glu can also be synthesized de novo from tricarboxcylic acid cycle intermediates (De Graaf et al. 2011). The rate of Glu release into the synapse and subsequent processes are dynamically modulated by neuronal and metabolic activity via stimulation of extrasynaptic Glu receptors, and it has been estimated that the cycling between Gln and Glu accounts for more than 80 % of cerebral glucose consumption (Sibson et al. 1998). The tight coupling between the Glu/Gln cycle and brain energetics is largely tied to the nearly 1:1 stoichiometry between glucose oxidation and the rate of astrocytic Glu uptake. This relationship was first determined by Magistretti et al. in cultured astroglial cells where the addition of Glu resulted in increased glucose consumption (Pellerin and Magistretti 1994). These results provided the hypothesis that glycolysis in the astrocytes results in a production of two molecules of ATP, which are then consumed by the formation of Glu from Gln, which suggests a tight coupling between the two mechanisms.

6.3.2 Glutamate and Glutamine Structure and Spectroscopy

The molecular structures of Glu and Gln are very similar and, as a result, give rise to similar magnetic resonance spectra (Govindaraju et al. 2000). The four protons from the two methylene

groups of glutamate Glu and Gln are located at 2.04–2.35 ppm and 2.12–2.46 ppm, respectively. Similarly, the methine group resonates at 3.74 ppm and 3.75 ppm for glutamate Glu and Gln, respectively. Thus, even though Glu has a relatively high concentration in the brain, its major resonances are usually contaminated by contributions from Gln, GABA, glutathione (GSH), and NAA. To avoid confusion in spectral assignment of Glu and Gln, the term "Glx" has traditionally been used to reflect the combined Glu and Gln concentrations. However, this approach does not allow for the evaluation of conditions where the concentrations of Gln and Glu are in opposing directions, nor does this approach allow for the evaluation of Gln and Glu separately. As our understanding of the importance of Glu/Gln system in the human brain has increased, much endeavor has been invested in being able to quantify Glu or Gln separately. The sections below detail methods for measuring Glu utilizing various pulse sequences to achieve the separation of Glu from co-resonating metabolites.

6.3.3 Single Voxel MRS and LCModel

LCModel (Provencher 1993) is a software package often used for post-processing of MRS data. It utilizes prior knowledge in the form of a basis set that is made up of a linear combination of in vitro, or simulated, spectra from individual metabolite solutions. The advantage of this method is that it is almost completely automated and utilizes algorithms for baseline correction and peak fitting without imposing restrictive parameterization and without subjective input. It is often used in the literature to calculate concentrations of individual metabolites including Glu and Gln. LCModel provides a quantitative measure of the accuracy of the measure by using the estimated standard deviations or Cramer–Rao lower bound (CRLB) that provides a measure of how reliable the measurement is. A standard deviation of <20 % has been used throughout the literature as the criteria for adequate reliability. While Glu standard deviation measures tend to fall below 20 %, Gln standard deviation measures do not. Given the overlap between the two molecules, it is unclear whether LCModel can accurately discern Glu from Gln.

In our lab we conducted a series of experiments where different solutions, or phantoms, were created that had different concentrations of Glu and Gln. In three of the phantoms, Glu was increased from 6 to 18 mM concentrations and Gln was maintained at 6 mM, which is equivalent to the physiological concentrations in the brain (3–5.8 mM (Govindaraju et al. 2000)). In the other three phantoms, Glu was maintained at 12 mM (equivalent to in vivo concentrations of 6–12.5 mM (Govindaraju et al. 2000)), but Gln was increased from 3 to 12 mM. Spectra were then acquired from these solutions using a clinical MRI scanner (Siemens 3 T TIM Trio) using conventional PRESS MRS (echo time of 30 ms, repetition time of 2 s). LCModel was then used to calculate the concentrations of each phantom as shown in Fig. 6.5. Our results showed that the variable concentration of Gln has a direct effect on the reported Glu concentrations and therefore demonstrates that this method is not sufficient for discerning Glu from Gln.

6.3.4 Optimal Echo Time

In order to better separate Glu and Gln, the echo time can be altered to minimize the contribution of the Gln signal to the Glx complex. Schubert et al. (Schubert et al. 2004) were able to selectively detect C4 proton resonances of Glu using a PRESS sequence at 3 T with a TE of 80 ms and analyzing the data using both the time and the frequency domains with prior knowledge obtained from phantom spectra. Using this approach, in vivo spectral features were similar to in vitro Glu spectral features collected from a phantom, and Glu signal was well resolved and separated from major interferences, such as Gln and NAA. Similarly, Jang et al. acquired PRESS spectra at 1.5 T in vitro and in vivo at four TE values: 30, 35, 40, and 144 ms (Jang et al. 2005), with the resulting spectra analyzed with LCModel (Provencher

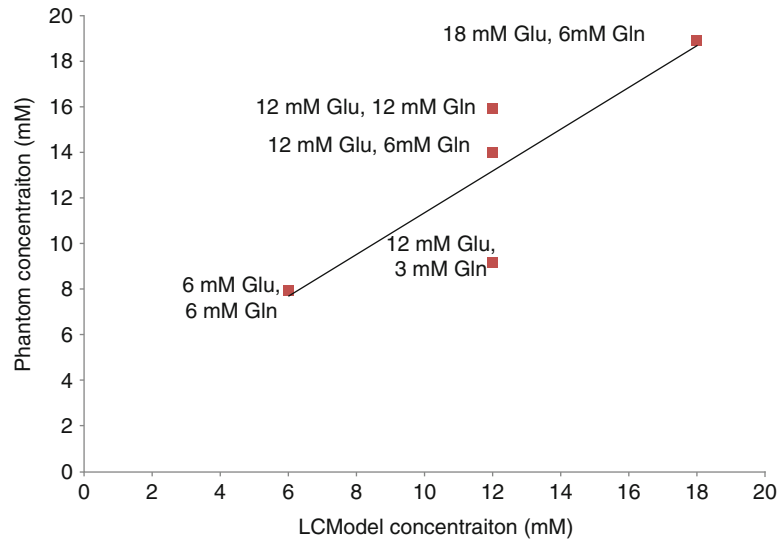

Fig. 6.5 Titration curve of solutions of glutamate and glutamine. Different concentrations of glutamate and glutamine were created as indicated by the data labels. The results show that the different concentrations of glutamine had a strong effect on the 12-mM Glu phantom solutions such that LCModel over- and underestimated the Glu concentration when Gln concentrations were high and low, respectively

2001). In vitro and in vivo spectra yielded the lowest Cramer–Rao lower bounds (CRLB) for Glu quantitation when TE was set to 40 ms. TE optimization for the purpose of Glu and Gln detection has also been demonstrated using stimulated echo acquisition mode (STEAM) spectroscopy by Yang et al. (2008), who optimized TE and mixing time (TM) to resolve the C4 proton resonances of Glu and Gln. Optimal TE methods are appealing acquisition strategies due to their ease of implementation for both acquisition and processing and the ease with which appropriate parameter timings can be selected at the scanner interface. Additionally, the resulting spectra can be analyzed using scanner software or commercially available software (e.g., LCModel, jMRUI) after simulating an appropriate basis set.

6.3.5 Ultrashort Echo Time

Due to the fact that Glu is a strongly coupled system, short echo time acquisitions are usually preferred over long echo time acquisitions for the purpose of reducing peak phase modulation. The ultrashort TE approach in such coupled systems gives rise to spectra where the majority of peaks are inphase and thus reduces signal cancellations due to J-modulations at longer echo times which in turn lead to more robust signal quantification. Wijtenburg and Knight-Scott (2011) quantified Glu/tCr at 3 T by combining short TE STEAM (6.5 ms) with phase rotation (Hennig 1992; Ramadan 2007) to detect Glu in human brain. This approach has been compared to 40 ms TE PRESS, 72 ms TE STEAM, and TE averaging and demonstrated that the short TE phase-rotation-STEAM approach yielded the greatest precision for Glu/tCr ratio quantification followed by TE averaging, PRESS 40 ms, and STEAM 72 ms (Wijtenburg and Knight-Scott 2011).

The implementation of very short echo time techniques requires substantial modification of standard vendor-supplied localization sequences. These spectra are usually complicated by a broad baseline extending over the whole spectral width, and care should be taken during analysis to eliminate the contribution of the baseline to the desired metabolite signal—which is usually done by utilizing T1 differences (Starcuk et al. 2001). The use of third-party spectral analysis software and, in some cases, the collection or simulation of metabolite basis set are essential to yield results of high accuracy (Wijtenburg and Knight-Scott 2011).

6.3.6 TE-Averaged PRESS

In this method, a number of 1D PRESS spectra are acquired at variable TE values and co-added

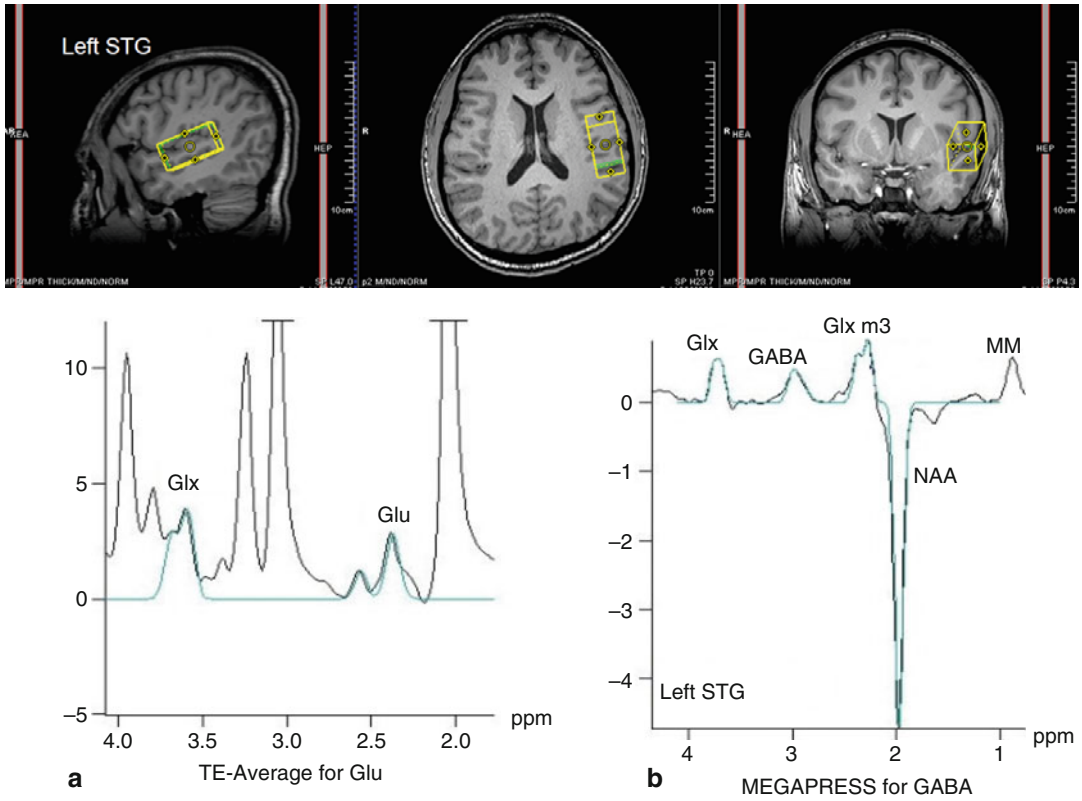

Fig. 6.6 In vivo spectra of schizophrenia. Representative spectrum of (**a**) glutamate-edited MRS (*left panel*) and (**b**) GABA-edited MRS (*right panel*) in the left superior temporal gyrus (*STG*) of a schizophrenia subject

(averaged) in real time to produce a single 1D, TE-averaged spectrum. Alternatively, the same TE-averaged spectrum can be obtained if these time-domain FIDs are ordered in a 2D matrix and a two-dimensional Fourier transform (2DFT) applied. The resultant 1D spectrum corresponding to the middle of the F1 axis (F1 = 0 Hz) is equivalent to the TE-averaged spectrum obtained above (Dreher and Leibfritz 1995; Bolan et al. 2002). This 1D spectrum offers relatively uncontaminated spectral peaks for C4 protons at 2.35 ppm for Glu and for C2 at 3.75 ppm for Glx (Hurd et al. 2004). Representative spectra are shown in Fig. 6.6a.

While TE averaging is a simple and reliable method for measuring Glu and Gln, it sacrifices spectral information arising from the J-evolution of other metabolites. The method also suffers from differential T2 weighting per individual TE value, which can be corrected for if a basis set is similarly simulated or experimentally acquired. TE-averaging sequences are not usually available from major MRI vendors but can be easily modified from standard PRESS sequence source code.

6.3.7 Glutamate Chemical Exchange Saturation Transfer (GLuCEST)

A large sensitivity enhancement for the detection of Glu can be achieved by careful design of MR exchange experiments. A recent example of this technique was recently implemented by Cai et al. where the chemical exchange saturation transfer (CEST) between bulk water and Glu was utilized for the detection of Glu (Cai et al. 2012). In such CEST experiments, advantage is taken from the protons on the Glu amine group, which are labile and in constant exchange with the protons of bulk water. When the Glu NH_2 protons are saturated

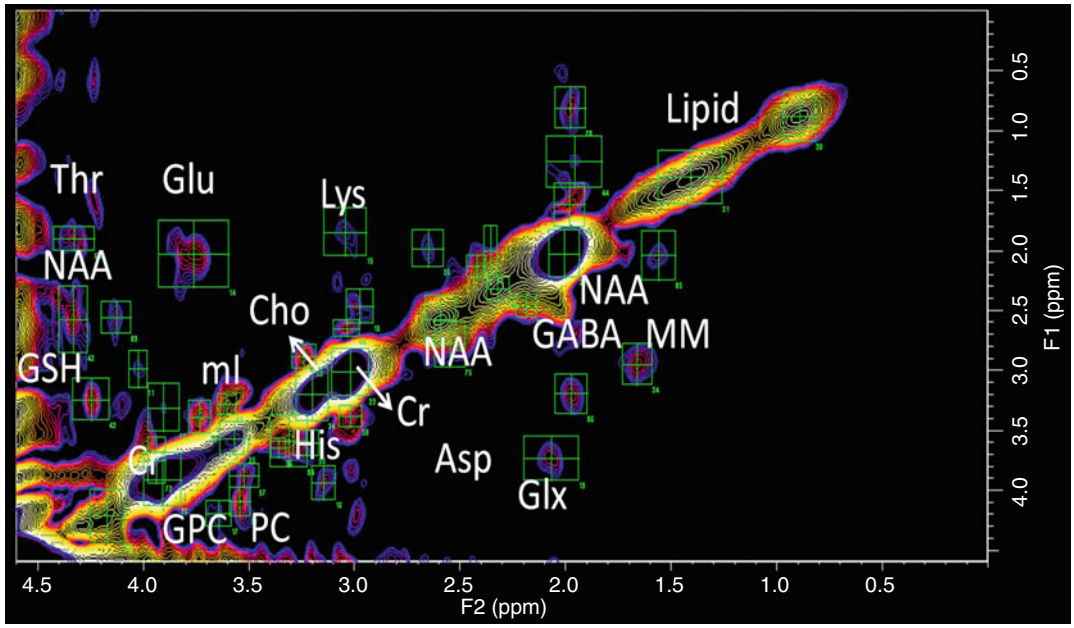

Fig. 6.7 2D correlated spectroscopy (COSY) of schizophrenia. Representative 2D COSY of left STG of SPD. *Green* ROIs show identification of multiple cross peaks such as threonine (*Thr*), *N*-acetylaspartate (*NAA*), glutathione (*GSH*), glutamate (*Glu*), myoinositol (*mI*), glycerophosphorylcholine (*GPC*), phosphorylcholine (*PC*), total choline (*Cho*), lysine (*Lys*), histidine (*His*), creatine (*Cr*), aspartate (*Asp*), gamma-amino butyric acid (*GABA*), glutamate–glutamine (*Glx*), macromolecules (*MM*), and lipids

by RF irradiation at 7.7 ppm (i.e., 3 ppm higher than water), the resultant saturation effect is transferred to water due to the ongoing chemical exchange between the protons of NH_2 and H_2O. This in turn leads to a reduction in the amplitude of water resonance due to the saturation of its protons and the saturation RF field applied to the Glu amine group. An excellent review of chemical exchange methodology can be found here (Zhou and van Zijl 2006).

6.3.8 Two-Dimensional MRS

An alternative to separating Glu from Gln is to use a second chemical shift dimension: 2D Fourier NMR spectroscopy utilizes a simple two-pulse sequence, 90x-t1-90x-Acq(t2), creating a dataset that is a series of one-dimensional (1D) spectra with traditional time readout (t2), but each with increments in delay (t1), inserted before the terminal readout 90° RF pulse (Jeener et al. 1979). Two-dimensional Fourier transformation (FT) of t1 and t2 produces a 2D spectrum where the x- and y-axes are the frequencies F2 and F1, respectively, known as correlated spectroscopy (COSY). In a 2D COSY spectrum, scalar coupling between protons in molecules results in cross peaks that allow for unambiguous identification of different metabolites (Thomas et al. 2001; Cocuzzo et al. 2011; Ramadan et al. 2011). This technology has been translated to clinical MR scanners and has been applied in vivo (Schulte et al. 2006), demonstrating detection of GABA, Glu, Gln, glutathione, as well as other metabolites (Fig. 6.7).

6.3.9 ^{13}C Spectroscopy

While the aforementioned methods have been utilized throughout the literature to study Glu, these measures provide static measures of Glu, measuring the total concentration of Glu in the brain without a sense of the dynamic changes that result from neurotransmission and brain energetics. Carbon 13 (^{13}C) MRS is presently

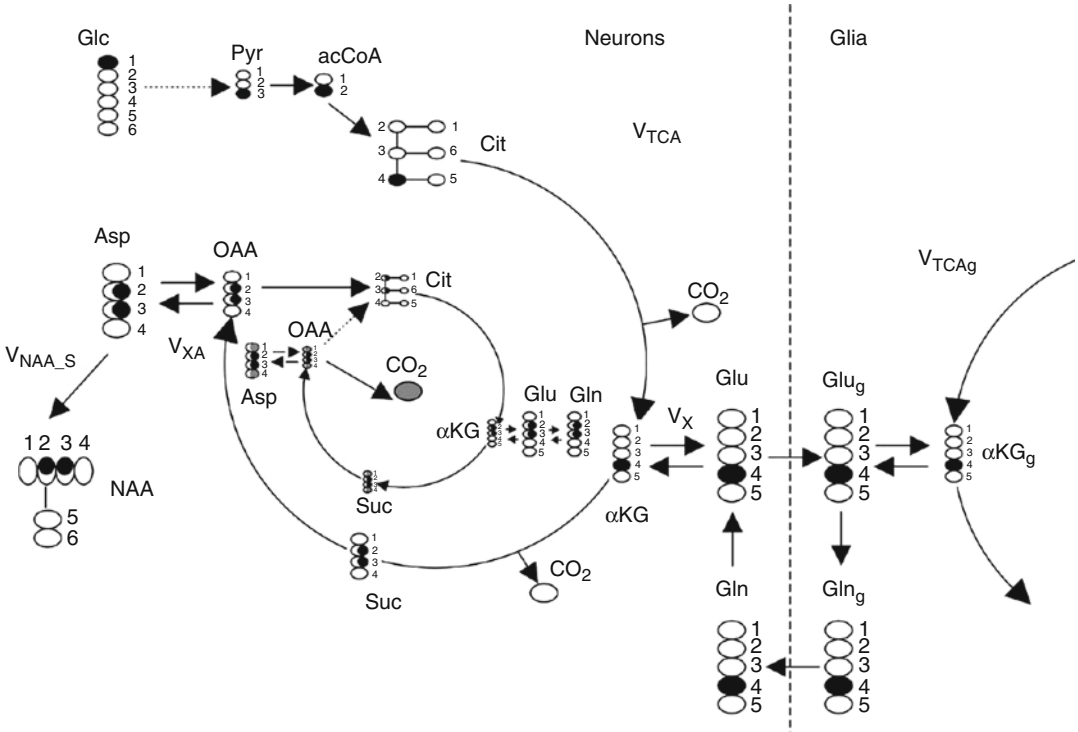

Fig. 6.8 Fate of 1-^{13}C atom of glucose through neuronal TCA and part of the neuronal–glial glutamate–glutamine cycle involved in glutamate neurotransmission. Two turns of the TCA cycle are represented. Carbon atoms enriched are shown in black. Carbons with 50 % chance of enrichment are shaded. For clarity the 3rd turn of neuronal TCA is represented only by bicarbonate ($^{13}CO_3$) release. In the paper, $^{13}CO_2$ is referred to as a bicarbonate ($H^{13}CO_3$). Other abbreviations: *Glc* glucose, *Pyr* pyruvate, *acetyl-CoA* acetyl coenzyme A, *Cit* citrate, V_{TCA} tricarboxylic acid cycle rate, *αKG* 2-oxoglutarate, $Vx_{,\alpha KG}$ Glu transaminase rate, V_{XA})transaminase or malate–aspartate shuttle rate, *Glu* glutamate, *Glug* glial glutamate, *Gln* glutamine, *Glng* glial glutamine, *αKGg* glial 2-oxoglutarate, *Suc* succinyl CoA, *OAA* oxaloacetate, *Asp* aspartate, *NAA* *N*-acetylaspartate, V_{NAA_S} NAA synthesis rate

the only method that provides noninvasive measurements of neuroenergetics and neurotransmitter cycling in the human brain. ^{13}C MRS, combined with the administration of ^{13}C-labeled substrates, allows the detection of ^{13}C incorporation from ^{13}C-labeled precursors into various carbon positions of metabolites, including the Glu cycles between neuronal and glial compartments (De Graaf et al. 2011). For example, if glucose, the primary fuel for the brain, is labeled with a nonradioactive isotope of ^{13}C on the first carbon, that label is retained as it is metabolized through the TCA cycle. At the point of alpha-ketoglutarate, the label is transaminated to Glu and Gln via the Glu/Gln cycle as shown in Fig. 6.8. As the label is incorporated separately into the fourth carbon group of Glu and Gln, real-time acquisition of the brain will result in the observation of the Glu C4and Gln C4 resonances at 34.4 ppm and 31.8 ppm, respectively. In the second turn of the TCA cycle, Glu C2 and C3 are labeled. Thus, ^{13}C MRS allows continuous, noninvasive monitoring of metabolic fluxes under different physiological or pathophysiological conditions.

The ^{13}C MRS acquisition consists of several different steps providing multiple means by which Glu can be measured. These include choice of substrate (glucose, acetate, label position), method of delivery (oral, IV, glucose clamped), data acquisition (direct detection, indirect detection), and method of analysis (dynamic difference spectroscopy, isotopomer

analysis) (Ross et al. 2003). It is important to note that the natural abundance of ^{13}C is approximately 1.1 % which implies that there is very little background signal of indigenous ^{13}C Glu, therefore providing excellent contrast to noise ratio of signals that arise from the incorporation of the ^{13}C label via the TCA cycle and subsequent transamination from alpha-ketoglutarate to the Glu/Gln cycle.

6.3.10 Glutamate in Psychiatric Diseases

6.3.10.1 Schizophrenia

It is thought that schizophrenia is related to a dysfunction in *N*-methyl-D-aspartate (NMDA) receptors, the major subtype of Glu receptors. Evidence from studies of NMDA receptor agonists such as phencyclidine and ketamine has shown decreased Glu levels as well as the psychotic symptoms observed in schizophrenia (Javitt and Zukin 1991). A recent meta-review (Marsman et al. 2013) examined 28 publications for a total of 647 patients with schizophrenia compared with 608 healthy controls appears to support this hypothesis by showing evidence of reduced Glu. While several brain regions were explored including the medial frontal region, hippocampus, and thalamus, only significant differences were found in the medial frontal region with reduced Glu. Group-by-age associations showed that Glu decreased at a faster rate with age in patients with schizophrenia compared to controls. While there have been few longitudinal studies of Glu using MRS, the literature appears to reflect that first-episode schizophrenics show increased glutamate whereas in the chronic stage of disease, Glu is decreased (Port and Agarwal 2011). This provides the basis for the second hypothesis of excitotoxicity of Glu in schizophrenia. Proponents argue that initially Glu levels are increased leading to excitotoxicity, which in turn leads to neuronal death as reflected by decreases in NAA. In the chronic stages of the disease, neuronal loss would also be reflected in decreases in Glu.

The meta-review also showed several studies where Gln is increased in schizophrenia (Marsman et al. 2013), which may reflect deficiencies in glutaminase, the enzyme that converts Gln into Glu, thus leading to decreased Glu and increased Gln as reflected in studies in chronic schizophrenia. However, it is unclear whether the methods used to measure Gln are accurate as few, if any, of the aforementioned pulse sequences have been validated for their measure of Gln given the overlap between Glu and Gln. The only efficient method that clearly delineates Gln from Glu are ^{13}C MRS studies of which there is only one published study (Harris et al. 2006) that showed reductions in TCA cycle rate, but did not show differences in Gln metabolism rates between schizophrenics and controls.

6.3.10.2 Dementia

Several proton spectroscopy studies have demonstrated decreases in Glu in Alzheimer's dementia using traditional MRS methods (Ross et al. 1997; Jones and Waldman 2004; Fayed et al. 2011) as well as others such as GluCEST (Cai et al. 2012, 2013). Reduced Glu is also found in HIV-related dementia (Ernst et al. 2010). Perhaps of greatest interest is that some studies in dementia patients have shown how Glu levels can be reversed using pharmaceutical interventions such as galantamine, a cholinesterase inhibitor, which showed that Glu increased after treatment in AD patients (Penner et al. 2010).

The role of Glu in Alzheimer's disease has also been explored in detail using ^{13}C MRS. The initial study in AD utilized [1-^{13}C] glucose in patients clinically diagnosed with AD as well as age-matched controls (Lin et al. 2003). The results of the study showed reduced Glu neurotransmission as measured by examining the time course of enrichment of Glu via the TCA cycle as well as relative enrichment of Glu to Gln. The time course measurements reflect the neuroenergetics of the brain and effectively measure TCA cycles rates. In AD patients, these rates were found to be reduced. The measure of Glu and Gln enrichment is of particular interest as it is reflective of Glu neurotransmission in itself. For example, if the glial TCA cycle is operating faster, then an enrichment pattern with relatively increased Gln signal versus Glu signal would be expected. In this study, Glu/Gln ratios were found to be significantly decreased, reflective of decreased neurotransmission. More interestingly, when correlated with NAA measures

as a surrogate marker for neuronal integrity, significant correlates were found with Glu/Gln ratios, further supporting the argument that this measure may be reflective of Glu neurotransmission in and of itself. As NAA, or the number of neurons decreased, Glu/Gln decreased, thus demonstrating that Glu neurotransmission may be decreased as a result in the reduction of the number of functioning brain cells. Sailasuta et al. also found that using [1-^{13}C] acetate, the third turn of the TCA cycle, which produces bicarbonate, is significantly slower in AD patients when compared to controls (Sailasuta et al. 2011).

6.3.10.3 Anxiety Disorders

Several studies have demonstrated that Glu is increased in the anterior cingulate cortex as a result of general (Strawn et al. 2013) and social anxiety disorder (Phan et al. 2005; Pollack et al. 2008) when compared with healthy controls. Excess Glu in anxiety is not only found in group differences and correlations with anxiety severity. One study showed that when anxiety is induced using cholecystokinin tetrapeptide, Glu levels in the anterior cingulate markedly increase within 2–10 min of the challenge (Zwanzger et al. 2013). Furthermore, when patients with anxiety are treated with medications, such as levetiracetam, Glu levels appear to decrease as a result of the treatment (Pollack et al. 2008).

6.3.10.4 Depression

A recent meta-review (Luykx et al. 2012) examined 16 publications of Glu in major depressive disorders (MDD) using MRS for a total of 281 patients and 301 controls. The anterior cingulate cortex and the prefrontal cortex were the two primary brain regions examined by most studies. The result of the meta-analysis showed that Glu and Glx were found to be significantly decreased in the anterior cingulate in MDD subjects. However, the literature remains mixed. For example, 2D COSY was used to study levels of metabolites in the dorsolateral prefrontal white matter regions to study MDD in the elderly. The study concluded that the depressed subjects had lower levels of NAA and higher levels of Glu/Gln, mI, and phosphoethanolamine (Binesh et al. 2004).

Perhaps the strongest evidence of the importance of using MRS to measure Glu in MDD comes from neuropharmacological literature where MRS has been used extensively to measure the effects of medication on brain metabolites. A recent review identified 15 articles where MRS was used to assess MDD treatments of which six specifically studied Glu and/or Glx. These findings showed several studies where Glx levels were initially decreased in MDD subjects, but after treatments such as electroconvulsive therapy and repetitive transcranial magnetic stimulation, Glx levels increased. These studies give rise to the hypothesis that Glu has a role in neuroplasticity (Sanacora et al. 2012), thus clearly demonstrate that Glx is an important component of MDD and that MRS is an effective means by which one can monitor therapeutic interventions.

6.3.10.5 Bipolar Disorder

Given the role of Glu in psychosis and depression, there is also a body of literature that has explored the use of MRS in bipolar disorder (BD). Similar hypotheses of Glu neurotoxicity and neuroplasticity arise in the literature for Glu MRS of BD as discussed in a recent review (Gigante et al. 2012), where 17 studies were identified. In most studies, the frontal lobe was the focus of MRS in regions such as the anterior cingulate cortex and the dorsal lateral prefrontal cortex. The meta-analysis showed elevated levels of Glx in BD. It is particularly interesting that this remained the case regardless of whether the patients were medicated. This is in contrast to MDD studies where Glx levels were decreased and modified by treatment.

6.4 γ-Amino Butyric Acid (GABA): Inhibitory Neurotransmitter

The counterpart to Glu is GABA, the major inhibitory neurotransmitter in the brain. Interestingly, in the developing brain, GABA is initially excitatory and later shifts to its inhibitory role as glutamatergic functions develop (Ben-Ari 2002). The balance between excitation and inhibition is reflected not only in the roles of these

two neurotransmitters but also in their metabolism as Glu is a metabolic precursor of GABA. GABA acts as an inhibitor by binding to specific receptors that open ion channels that allow for the flow in of negatively charged ions or the flow out of positively charged ions, thus creating a negative membrane potential. This, in turn, hyperpolarizes the cells and prevents the formation of action potentials. GABA is of particular interest given the availability of drugs that modulate the binding of GABA receptors, such benzodiazepines, which have helped elucidate the role of GABA across a broad range of psychiatric conditions such as anxiety, memory loss, depression, and pain. Similar to Glu, GABA is difficult to detect using MRS due to its overlap with the resonances of Glu and Gln, therefore requiring specific sequences to measure. Further, the concentration of GABA in the brain ranges from 1.3 to 1.9 mM (Govindaraju et al. 2000) and therefore is difficult to detect accurately and consistently given its low concentration.

6.4.1 GABA Metabolism

GABA is synthesized via the GABA shunt (Olsen and DeLorey 1999): first, alpha-ketoglutarate from the TCA cycle is transaminated to glutamic acid by GABA transaminase (GABA-T). Glutamic acid decarboxylase (GAD) catalyzes the decarboxylation of glutamic acid to GABA. GABA can be metabolized to succinic semialdehyde by GABA-T but only in the presence of alpha-ketoglutarate in order to conserve the supply of GABA. Finally, succinic semialdehyde is oxidized into succinic acid which then reenters the TCA cycle, thus completing the shunt. This metabolism takes place in the GABAergic neuron where GABA is released as a neurotransmitter and then binds to receptors on the postsynaptic neuron. There are three different types of GABA receptors, $GABA_A$, $GABA_B$, and $GABA_C$ (also considered $GABA_A$-ρ), which have different properties where A and A-ρ are fast-acting and B is slow acting and hence different pharmacologies and diseases. Finally, GABA can also be taken up by the astrocytes, thus leading to a GABA–glutamine cycle following similar metabolic pathways as the GABA shunt.

6.4.2 GABA Structure

As with Glu, the GABA nuclear spins *J*-couple with other neighboring spins. This causes the molecule to appear as a number of small peaks spread out a broad frequency range on a standard PRESS spectrum. This results in multiplet resonances around 1.9, 2.28, and 3.0 ppm. The problem with all of those locations is that they overlap with other major metabolites within the spectrum such as NAA at 2.02 ppm, Glu at 2.34 ppm, and Cr at 3.02 ppm. Therefore, specialized methods are once again required to discern GABA and to reliably estimate its concentrations in vivo.

6.4.3 MEGA-PRESS

One technique to measure the GABA peaks involves utilizing a difference of spectra that selectively preserves the GABA signal while eliminating other metabolites. GABA has characteristic resonances at 3.0 and 1.9 ppm. A frequency-selective pulse that targets one of these regions would also enhance the signal in the other region due to the effect of *J*-coupling. Applying a frequency-selective pulse that is on resonance at 1.9 ppm would increase the signal in the 3.0 ppm region if GABA is indeed present. Likewise, a frequency-selective pulse that is off resonance would not have an effect on the 3.0 ppm peak. Subtracting the spectra from these two different pulse acquisitions should preserve the metabolite that only resonates at the characteristic frequencies of GABA as shown in Fig. 6.6b. MEGA-PRESS utilizes these frequency-selective pulses and combines them with PRESS localization. While this method has the selectivity to measure GABA, by utilizing difference spectra, there is a loss in SNR and a chance to introduce additional artifacts as a result of subtraction.

This method has been successfully applied to estimate the GABA concentration of several brain regions including the anterior cingulate cortex (ACC), occipital lobe, and parietal lobe (Terpstra

et al. 2002; Öz et al. 2006; Bhattacharyya et al. 2007; Edden and Barker 2007; Kaiser et al. 2007; Waddell et al. 2007). This sequence combined with LCModel quantitation of the MEGA-PRESS spectra can provide an estimate of the absolute GABA concentration present in the brain in vivo.

6.4.4 Double Quantum Coherence (DQC)

A DQC filter technique can be used to eliminate uncoupled resonances from metabolites like choline, creatine, and NAA and leave strongly coupled resonances from GABA in a single acquisition without the need for subsequent spectral editing. This method exploits the difference in the phase-accumulation rate of coherences from single versus multiple quantum states. By selectively rephasing, only the magnetization from a multiple quantum coherence, the signal from the uncoupled metabolites, is removed. Because this method does not require the difference spectra from two scans, the SNR is improved and the acquisition time is reduced (Keltner et al. 1997). Quantifying GABA from DQC-filtered spectra has the potential to provide more reliable and reproducible estimates (McLean et al. 2002; Choi et al. 2004, 2005a, b). The technique can be applied with PRESS localization just as with MEGA-PRESS, and the same applications of study are possible. Comparison of subjects with occipital lobe epilepsy (OLE) versus healthy controls shows increased levels of GABA acquired from DQC spectra (Simister et al. 2003). An increased GABA concentration after treatment with the SSRI citalopram in the OCC with healthy subjects is also detected with DQC spectra (Bhagwagar et al. 2004).

6.4.5 2D JPRESS

Similar to 2D COSY, 2D JPRESS also acquires a series of TE increments to provide a 2D MR spectrum. 2D JPRESS differs from 2D COSY in that it utilizes the standard PRESS sequence for each increment with the addition of maximum echo sampling scheme that increases the sensitivity of the method (Ke et al. 2000; Schulte et al. 2006; Lymer et al. 2007). Additional consideration is also necessary to quantify the 2D JPRESS spectra. Unlike COSY where the cross-peak volumes can be measured as an analog of metabolite concentration, 2D JPRESS cross peaks are not as differentiated and therefore do not lend itself as readily for visual analysis. More sophisticated tools like ProFit (Schulte and Boesiger 2006) attempt to quantify the 2D spectra with prior knowledge basis sets of the metabolites similar to LCModel.

2D JPRESS can also be combined with the CSI method previously described in Sect. 2.3 where instead of using PRESS, 2D JPRESS is used instead (Jensen et al. 2005). 2D-JPRESS CSI can sample many regions of interest to determine the GABA concentration, but obtaining reliable spatial distribution maps of GABA in the brain requires overcoming technical challenges. The smaller voxel size greatly reduces the SNR of each spectrum making the GABA concentration estimates inherently less reliable relative to estimates from larger voxels. The 2D JPRESS can also be combined into a 1D TE-averaged JPRESS spectrum, as described earlier; however, while the TE-averaged JPRESS spectra can be used to reliably estimate other metabolites like Glu, this method is less reliable for quantifying GABA (Mullins et al. 2008).

6.4.6 GABA in Psychiatric Disease

6.4.6.1 Schizophrenia

Alterations in GABA neurotransmission underlying the pathophysiology of schizophrenia are evidenced by reduced GABA synthesis as reflected by decreased activity of GAD67 in parvalbumin-staining cortical neurons (Gonzalez-Burgos et al. 2010). Additionally, $GABA_A$ receptors may be upregulated, possibly reflecting a compensatory response to reduced GABA levels (Jarskog et al. 2007). Due to the relatively recent advances in MRS that has allowed for GABA measurements, MRS studies of GABA in schizophrenia are rapidly evolving. A study of chronic schizophrenics reported the MEGA-PRESS estimated GABA to be 10 % lower than in healthy controls and to

correlate with the orientation-specific surround suppression – a quantitation of the level of visual inhibition that is thought to be regulated by GABAergic pathways (Yoon et al. 2010). A more recent study found similar reduction of GABA in chronic schizophrenia in the anterior cingulate which also correlated with poor attention performance (Rowland et al. 2012). In a study in early course schizophrenia, decreased GABA levels in the basal ganglia was also found (Goto et al. 2009). In contrast, however, another study found increases in GABA/Cr ratios in chronic SZ (Ongür et al. 2010). These discrepant results may have resulted from the use of Cr as studies have shown that Cr is reduced in schizophrenia thus possibly elevating the ratio if the reduction is greater than the reduction in GABA. It is also clear that there are significant medication effects on the GABA measures as another study in schizophrenia showed that the measured GABA concentration in the anterior cingulate was significantly negatively correlated with the dose of antipsychotics (Tayoshi et al. 2010). In this study, exclusion of patients on these compounds abolished the statistically significant effects.

6.4.6.2 Anxiety

There have only been a handful of studies that have used MRS for measuring GABA in anxiety. Comparing patients with panic disorder and healthy controls, MRS studies have found that GABA is reduced in the occipital cortex, anterior cingulate cortex, and medial prefrontal cortex (Goddard et al. 2001; Long et al. 2013). Interestingly, upon administration of benzodiazepine, GABA levels in the occipital cortex did not change (Goddard et al. 2004). Other studies however have not found differences in GABA levels in patients with panic disorder in the dorsal prefrontal or ventrolateral prefrontal regions (Hasler et al. 2005). Similarly, there were no significant differences in patients with social anxiety disorder (Pollack et al. 2008). It should be noted however that measuring GABA is challenging and can often result in large variability in the measurement which would result in the lack of significant findings, but should not necessarily be interpreted as a lack of change in GABA.

6.4.6.3 Depression

A recent review cited 14 papers that utilized MRS to measure GABA levels in major depressive disorder where there are general findings of decreased GABA in the occipital cortex, anterior cingulate, and dorsal prefrontal cortex but not in the frontal white matter (Maddock and Buonocore 2012). Furthermore, the review highlights four studies that examine the effect of treatment on GABA levels and show that treatments of selective serotonin reuptake inhibitors and electroconvulsive therapy both increased levels of GABA in the occipital cortex, although one study of cognitive–behavioral therapy did not show increased levels.

6.4.6.4 Bipolar Disorder

Two studies have shown that patients with bipolar disorder (BD) exhibit lower GABA in the anterior cingulate, parieto-occipital cortex, and occipital cortex (Bhagwagar et al. 2004; Brady et al. 2013). A CSI study, however, did not show any significant differences between patients with BD and healthy controls (Kaufman et al. 2009). It is likely that the low SNR of CSI sequences, as described earlier, resulted in the lack of statistical differences between the two cohorts.

6.5 Glutathione (GSH)

The primary role of GSH is as an antioxidant, providing the brain's defense system against damaging reactive oxygen species (ROS) that arise from oxidative stress such as super oxide, nitric oxide, hydrogen peroxide, and free radicals (Dringen et al. 2000). The damage caused by ROS include DNA modification, lipid peroxidation, and protein modification from which the brain is especially vulnerable due to the large quantity of ROS produced there, availability of lipids, and iron deposition that catalyzes ROS reactions. Oxidative stress is also strongly associated with neuroinflammatory processes (Mosley et al. 2006; Agostinho et al. 2010). As a result, compromises in GSH metabolism have been found to play an important role in the pathogenesis across a wide

variety of diseases such as neurodegenerative disorders as well as psychiatric disorders.

6.5.1 Glutathione Metabolism

GSH is synthesized intracellularly by first combining Glu and cysteine to form γ-glutamylcysteine via synthetase enzyme followed by addition of glycine as catalyzed by GSH synthetase. Due to the limited supply of Glu, cysteine, and glycine, in different cell types, GSH is synthesized between different neurons, astrocytes, and glial cells, thus providing an interesting specificity to GSH measures to processes such as neuroinflammation. The thiol group on GSH is a reducing agent in that it can donate an electron to unstable molecules such as ROS. When ROS is present, GSH will reduce ROS by catalysis of glutathione peroxidase (GPx) to form glutathione disulfide (GSSG). GSSG can then regenerate GSH using glutathione reductase. GSSG resonates at a different frequency on the MRS spectrum (Satoh and Yoshioka 2006) and therefore reductions in GSH concentrations as measured by MRS would provide a putative measure of brain oxidative stress and neuroinflammation. However, it is important to note that defects in GSH metabolism can also reduce concentrations of GSH, and disruptions to GSH synthesis or GSH peroxidation can also reflect oxidative stress.

6.5.2 Measuring Glutathione

As a tripeptide of Glu, cysteine, and glycine, the GSH spectrum will have overlap with all three of those metabolites (Matsuzawa and Hashimoto 2011). From the Glu moiety, the methylene protons give rise to multiplets at 2.15–2.55 ppm and the methine at 3.77 ppm (which also has contributions from the glycine moiety). The cysteine moiety of GSH gives rise to resonances at 4.56, 2.93, and 2.98 ppm. Thus, there is significant overlap between Glu and GSH resonances. This is particularly of concern given that GSH concentrations in the brain are 1–3 mM, whereas Glu concentrations are 6–10 mM (Govindaraju et al. 2000). Furthermore, there is also overlap with NAA and creatine resonances as well. Fortunately, many of the same tools that are used for separating Glu and GABA from overlapping resonances can also be used for GSH. Minor modifications to those methods are required:

6.5.2.1 LCModel

Some studies have reported measuring GSH using conventional PRESS or STEAM MRS methods by using LCModel (Terpstra et al. 2005; Wood et al. 2009; Hermens et al. 2012; Lagopoulos et al. 2013; Duffy et al. 2013). Current versions of the LCModel basis set (versions 6.2 and above) contain glutathione within the basis set which can be used for quantifying levels of GSH in the brain. However, similar to the issue described for Glu and Gln, GSH measures are often reported to have <20 % CRLB in most publications; however; once again, our laboratory tests have shown that the Glu concentration can have a significant impact upon the estimation of the GSH concentration despite the fact that the CRLB are still reported to be less than 20 %. It is therefore unclear whether or not this is a reliable method by which one can measure GSH. Furthermore, it is important that those studies that utilize this method must report the CRLB and they should be below 20 %.

6.5.2.2 MEGA-PRESS

In this implementation of the pulse sequence, the selective editing pulses are targeted to the α-cysteinyl protons of GSH at 4.56 ppm, which after subtraction of the on and off resonance acquisitions results in detection of the β-cysteinyl protons of GSH (Choi et al. 2004; Terpstra et al. 2005; Matsuzawa et al. 2008; Mandal et al. 2012). LCModel is then used to fit this resonance. Unlike the PRESS or STEAM spectra, the spectral editing removes the contributions of metabolites such as Glu and Gln and thus provides a more accurate measure of GSH concentrations (Fig. 6.9).

6.5.2.3 Double Quantum Coherence

Similarly, DQC methods can also be modified to target the GSH molecule. In the one study reviewed here, the group also focused on the cysteinyl groups.

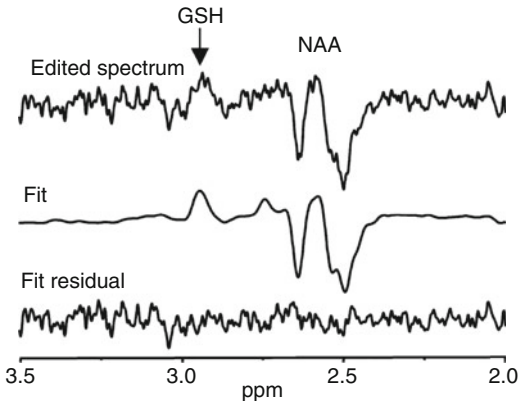

Fig. 6.9 MEGA-PRESS GSH spectrum. Representative spectrum of glutathione measured by MEGA-PRESS. The difference spectrum is shown at the *top*, with an *arrow* pointing to the GSH resonance. The *middle* spectrum shows the fit of the data and the bottom spectrum shows the residual. Note the NAA is co-edited with this implementation of the MEGA-PRESS sequences (Terpstra et al. 2005)

6.5.2.4 2D MRS

Although not utilized yet in psychiatric studies, 2D JPRESS and 2D COSY methods can accurately measure GSH in the brain (Thomas et al. 2001; Schulte et al. 2006). The advantage of the 2D methods is that unlike MEGA-PRESS or DQC which can only measure a single metabolite for one acquisition, 2D JPRESS and COSY can measure many metabolites. For example, in order to measure Glu, GABA, and GSH, using 1D methods would require three separate acquisitions of approximately 7 min each for a total of 21 min. 2D MRS could measure those metabolites and more in 12 min (Ramadan et al. 2011).

6.5.3 Glutathione in Psychiatry

6.5.3.1 Schizophrenia

A recent review identified four studies that measure GSH in patients with schizophrenia (Matsuzawa and Hashimoto 2011). The first study used DQC to measure GSH in the medial prefrontal cortex in 14 patients including schizophrenia and schizophreniform disorder and compared them to 14 controls (Do et al. 2000). GSH was found to be significantly lower which was further confirmed by a decrease in CSF GSH levels. The second study utilized MEGA-PRESS and STEAM in the medial prefrontal cortex in 11 patients with schizophrenia and 9 controls, and although they found decreased GSH, the difference was not statistically significant between the two groups (Terpstra et al. 2005). The third study also utilized MEGA-PRESS in the medial prefrontal cortex, and although they too did not find significant group differences between schizophrenic ($n=20$) and controls ($n=16$), they did find significant negative correlations between GSH measures and negative symptom scores (Matsuzawa et al. 2008). Finally, the fourth study utilized LCModel with conventional PRESS (TE = 30 ms) in the bilateral temporal cortex in first-episode psychosis ($n=30$), of which 13 were neuroleptic naïve and had various diagnoses of schizophrenia, schizopsychosis, schizoaffective disorder, and depression with psychotic symptoms (Wood et al. 2009). Their findings are surprisingly contrary to previous studies where they show increased GSH in the schizophrenia group when compared with controls. It is important to note however the authors used the criteria of <50 % CRLB which indicates that metabolite concentrations could range from zero to twice the estimated concentration. According to the LCModel guidelines, this would imply that the metabolite is undetectable. Coupled with findings of interference of Glu with GSH LCModel measures, it is likely that these results are not reliable.

6.5.3.2 Dementia

Two recent studies have utilized MRS to measure GSH in dementia. The first study utilized MEGA-PRESS and measured GSH in healthy young and old controls, 11 patients diagnosed with MCI, and 14 patients that suffered from Alzheimer's disease (Mandal et al. 2012). They explored several different brain regions including the frontal cortex, parietal cortex, hippocampus, and cerebellum. While the study found higher GSH in the young controls versus the elderly controls and patients, there did not seem be any significant differences between the elderly controls and MCI or AD patients. The second study

(Duffy et al. 2013), however, examined a much larger group of subjects (54 MCI and 41 healthy controls) using PRESS (TE = 35 ms), MRS, and LCModel in the anterior and posterior cingulate gyri. They found elevated GSH levels in MCI patients when compared to age-matched healthy subjects in both brain regions. Furthermore, they also found the anterior and posterior cingulate GSH levels negatively correlated with executive and memory function, respectively. The authors hypothesize that the increased GSH may be a neuroprotective affect that arises from the upregulation of GSH in response to oxidative stress onset by MCI.

6.5.3.3 Bipolar Disorder

Fifty-four patients with bipolar disorder (13 bipolar I, 25 bipolar II, 15 bipolar spectrum) and 51 age- and gender-matched controls were studied with PRESS (TE- = 30 ms) in the anterior cingulate cortex and GSH measured using LCModel (Lagopoulos et al. 2013). In this case, CRLB was reported to be less than 20 %. There were no significant differences found in the comparison of BD patients and controls nor were there any significant correlations with clinical scores of depression or mania. The authors conclude that oxidative stress does not play a role in bipolar disorder. It is interesting that an earlier paper from the same group utilizing the same methods but in a larger cohort ($n = 80$; mixed psychiatric disease including depression, bipolar, and psychosis) found that GSH was accounted for by the 40 % of the clusters when cluster analysis was applied (Hermens et al. 2012). One of the clusters exhibited higher GSH; however, as a mix of different psychoses, it is difficult to determine the underlying pathophysiology, which might explain this finding.

6.6 Other Metabolites

The following metabolites can be measured using conventional MRS techniques. A description of their role in the brain and how they are affected by various psychiatric diseases will be described.

6.6.1 Creatine (Cr)

The major resonance at 3.02 ppm is comprised of creatine (Cr) and phosphocreatine (PCr), although in general, most publications refer to the combination as Cr. LCModel provides both a Cr measure and a PCr measure, although conventional proton MRS cannot readily distinguish Cr from PCr as they are in rapid molecular exchange with one another. Instead, ^{31}P MR spectroscopy must be used to discern the phosphorous resonances in PCr. The metabolism of Cr and PCr provided the basis of energy metabolism in the brain via the mitochondria where Cr is phosphorylated by the enzyme creatine kinase and adenosine triphosphate (ATP) to form PCr in reverse (Ross 2000). Used to maintain energy homeostasis in the brain, Cr is fairly uniform in different areas of the brain and between subjects and therefore is often used as a normalization factor between metabolites and subjects such that a ratio to Cr is often used. The danger of utilizing such a ratio is that it naturally assumes that the concentration of Cr in the brain (approximately 8 mM) is static and unaffected by disease (Kreis et al. 1993).

In many situations, this is not the case as energy utilization can be affected by disease and other Cr metabolic pathways. Mitochondrial dysfunction in the brain would likely cause changes in Cr and PCr and has been implicated across a range of neuropsychiatric disorders including schizophrenia and bipolar disorder (Rezin et al. 2009). ^{31}P MRS studies have shown reduced PCr in schizophrenia (Kegeles et al. 1998; Blüml et al. 1999) which supports findings from proton MRS studies where reduced Cr has been found using TE-averaged PRESS in schizophrenia (Ongür et al. 2009). Interestingly in the same study, bipolar disorder did not show changes in PCr; however, other studies using both proton MRS (Frey et al. 2007) and ^{31}P MRS (Kato et al. 1994) have shown reductions in Cr and PCr. Findings of changes in Cr in schizophrenia and bipolar disorder however are inconsistent. A recent study showed that meta-analysis failed to find significant abnormalities in Cr levels in both diseases (Kraguljac et al. 2012).

It is also important to note that in addition to mitochondrial dysfunction, Cr can be affected by other factors. For example, Cr is synthesized in the liver, and therefore, patients with liver failure will result in reduced Cr in the brain. Cr is also an osmolyte and therefore can be affected by osmotic equilibrium in the brain (Bluml et al. 1998). It is therefore important to screen for comorbid diseases such as liver disease and other conditions that may cause changes in brain metabolites secondary to the disease of interest.

6.6.2 Choline (Cho)

Similar to Cr, Cho is a term that includes several different metabolites that contain the choline moiety that give rise to the primary resonance at 3.2 ppm. These metabolites include choline, phosphorylcholine (PC), and glycerophosphorylcholine (GPC), which are the main constituents, as well as phosphorylethanolamine and glycerophosphorylethanolamine, to a lesser extent. All of these metabolites are constituents of sphingomyelin and lecithin which make up the myelin sheath critical for the propagation of signals throughout the brain. As a result, increased Cho is found in areas of greater myelin and membrane density such as in the white matter and in the pons. In addition, PC and GPC are involved in the metabolism of phosphatidylcholine and other membrane phospholipids. PC is a precursor of membrane phospholipid synthesis, and GPC is produced upon the breakdown of membrane phospholipids. Thus, the turnover of the membrane of myelin phospholipids as well as demyelination are closely tied to increases in Cho as observed by MRS. As a result of the involvement of Cho in both membrane turnover and degradation as well as density, it is a sensitive marker but not necessarily specific to membrane conditions.

Recent reviews in Alzheimer's dementia (Kantarci 2007), schizophrenia (Kraguljac et al. 2012), and depression (Caverzasi et al. 2012) have shown conflicting reports on Cho levels in these diseases. It is only in bipolar disorder where the literature has shown consistent elevated choline signal in the basal ganglia (Maddock and Buonocore 2012). The most likely reason for why Cho findings are discordant across different studies within the same disease is due to the sensitivity of Cho to the gray and white matter volumes in the regions of interest studied. For example, a meta-analysis has shown that duration of illness is associated with basal ganglia gray matter volume in bipolar patients (Bora et al. 2010), which may explain the increase in Cho as a function of membrane density. Within studies, Cho levels could be affected by placement of the voxel for MRS, which may include different volumes of gray and/or white matter when comparing controls with patients thus resulting in conflicting reports of Cho changes. The solution to this problem is to combine image segmentation within the voxel of interest for MRS to account for the relative contributions of gray and white matter to the Cho level.

6.6.3 Myoinositol (mI)

mI is a simple sugar alcohol; however, it is involved in a multitude of different metabolic processes, and as a result, its role cannot be defined to a single function (Ross and Bluml 2001). It is a cerebral osmolyte and also believed to be an astrocyte marker. Similar to Cho, mI has also been implicated in demyelination. While its role may not be well understood, the importance of mI however is the broad range of concentrations found across different conditions from 3× the normal adult values in newborns to nearly zero in hepatic encephalopathy. It has been found to be highly specific and sensitive within the context of disease diagnosis in patients when compared with controls and therefore provides great clinical value.

The importance of mI has long been recognized in studies of dementia. In early stages of dementia such as mild cognitive impairment, mI is elevated long before symptoms of dementia are obvious (Kantarci 2013). As described earlier in Sect. 2.5.2, mI in combination with NAA predicted outcome of MCI in patients and is also highly sensitive and specific in the diagnosis of Alzheimer's disease where much of the specificity arose from mI measures.

There does not appear to be strongly associated changes in mI in other psychiatric disorders including schizophrenia, bipolar disorder, or depression.

It should be noted that like Glu, mI can only be observed at short echo times (TE < 55 ms), and so studies that utilize long echo time MRS would not be capable of measuring mI. Also, given the changes in mI observed in hepatic encephalopathy, it is important to screen for liver disease to ensure that changes in mI are not masked by comorbid conditions.

Conclusion

MRS is a powerful neuroimaging tool that can provide noninvasive, quantitative, and objective measures of key neurometabolites *in vivo*. This insight can be utilized to reveal the underlying pathology of many neuropsychiatric disorders. Highly complementary to other imaging tools, MRS can be used in conjunction to better understand the different brain functions such as neurodegeneration (NAA), excitotoxicity (Glu), inhibition (GABA), neuroinflammation (GSH), mitochondrial function (Cr), membrane turnover and demyelination (Cho), and gliosis (mI). In schizophrenia, reduced NAA, increased Gln, and variable Glu (dependent on chronicity, reduced GABA, GSH, and Cr) have been the major findings providing insight into the neuronal function and the influence of the major neurotransmitters upon the disease. In dementia, the primary findings are reduced NAA and Glu and increased mI, which are not only diagnostic for Alzheimer's disease but also in predicting progression of dementia as well. Reduced NAA, Glu, and GABA are characteristic of depression. Those results provide an interesting contrast to bipolar disorder where NAA and GABA are also reduced but Cho and Glu are increased and GSH does not appear to change. Anxiety disorder is probably the least explored by MRS but have shown increased Glu but decreased GABA, thereby demonstrating an imbalance between the major excitatory and inhibitory neurotransmitters in the brain. As MRS methods evolve through the various pulse sequences and post-processing methods that are more and more rapidly becoming available to neuroscientists, psychiatrists, psychologists, and physicians, MRS may eventually cross over into the realm of clinical diagnosis where it would be a valuable tool to provide mechanistic and physiological insight into psychiatric diseases much as genetics and pathophysiology have provided for other diseases.

References

Agostinho P, Cunha RA, Oliveira C (2010) Neuroinflammation, oxidative stress and the pathogenesis of Alzheimers disease. Curr Pharm Des 16:2766–2778. doi:10.2174/138161210793176572

Andrew ER (1980) N.m.r. imaging of intact biological systems. Philos Trans R Soc Lond B Biol Sci 289:471–481

Bak LK, Schousboe A, Waagepetersen HS (2006) The glutamate/GABA-glutamine cycle: aspects of transport, neurotransmitter homeostasis and ammonia transfer. J Neurochem 98:641–653. doi:10.1111/j.1471-4159.2006.03913.x

Barker PB (2001) N-acetyl aspartate – a neuronal marker? Ann Neurol 49:423–424

Baslow MH (2000) Functions of N-acetyl-L-aspartate and N-acetyl-L-aspartylglutamate in the vertebrate brain: role in glial cell-specific signaling. J Neurochem 75:453–459

Baslow MH (2010) Evidence that the tri-cellular metabolism of N-acetylaspartate functions as the brain's "operating system": how NAA metabolism supports meaningful intercellular frequency-encoded communications. Amino Acids 39:1139–1145. doi:10.1007/s00726-010-0656-6

Ben-Ari Y (2002) Excitatory actions of gaba during development: the nature of the nurture. Nat Rev Neurosci 3:728–739. doi:10.1038/nrn920

Bhagwagar Z, Wylezinska M, Taylor M et al (2004) Increased brain GABA concentrations following acute administration of a selective serotonin reuptake inhibitor. Am J Psychiatry 161:368–370

Bhattacharyya PK, Lowe MJ, Phillips MD (2007) Spectral quality control in motion-corrupted single-voxel J-difference editing scans: An interleaved navigator approach. Magn Reson Med 58:808–812

Binesh N, Kumar A, Hwang S et al (2004) Neurochemistry of late-life major depression: a pilot two-dimensional MR spectroscopic study. J Magn Reson Imaging 20:1039–1045. doi:10.1002/jmri.20214

Blüml S, Tan J, Harris K et al (1999) Quantitative proton-decoupled 31P MRS of the schizophrenic brain in vivo. J Comput Assist Tomogr 23:272–275

Bluml S, Zuckerman E, Tan J, Ross BD (1998) Proton-decoupled 31P magnetic resonance spectroscopy reveals osmotic and metabolic disturbances in

human hepatic encephalopathy. J Neurochem 71:1564–1576
Bolan PJ, DelaBarre L, Baker EH et al (2002) Eliminating spurious lipid sidebands in 1H MRS of breast lesions. Magn Reson Med 48:215–222
Bora E, Fornito A, Yücel M, Pantelis C (2010) Voxelwise meta-analysis of gray matter abnormalities in bipolar disorder. Biol Psychiatry 67:1097–1105. doi:10.1016/j.biopsych.2010.01.020
Bottomley PA (1987) Spatial localization in NMR spectroscopy in vivo. Ann N Y Acad Sci 508:333–348
Brady RO, McCarthy JM, Prescot AP et al (2013) Brain gamma-aminobutyric acid (GABA) abnormalities in bipolar disorder. Bipolar Disord. doi:10.1111/bdi.12074
Cai K, Haris M, Singh A et al (2012) Magnetic resonance imaging of glutamate. Nat Med 18:302–306. doi:10.1038/nm.2615
Cai K, Singh A, Roalf DR et al (2013) Mapping glutamate in subcortical brain structures using high-resolution GluCEST MRI. NMR Biomed. doi:10.1002/nbm.2949
Capizzano AA, Jorge RE, Acion LC, Robinson RG (2007) In vivo proton magnetic resonance spectroscopy in patients with mood disorders: a technically oriented review. J Magn Reson Imaging: JMRI 26:1378–1389. doi:10.1002/jmri.21144
Caverzasi E, Pichiecchio A, Poloni GU et al (2012) Magnetic resonance spectroscopy in the evaluation of treatment efficacy in unipolar major depressive disorder: a review of the literature. Funct Neurol 27:13–22
Chakraborty G, Mekala P, Yahya D et al (2001) Intraneuronal N-acetylaspartate supplies acetyl groups for myelin lipid synthesis: evidence for myelin-associated aspartoacylase. J Neurochem 78:736–745
Choi I-Y, Lee S-P, Merkle H, Shen J (2004) Single-shot two-echo technique for simultaneous measurement of GABA and creatine in the human brain in vivo. Magn Reson Med 51:1115–1121. doi:10.1002/mrm.20082
Choi I-Y, Lee S-P, Shen J (2005a) In vivo single-shot three-dimensionally localized multiple quantum spectroscopy of GABA in the human brain with improved spectral selectivity. J Magn Reson (San Diego, Calif : 1997) 172:9–16. doi:10.1016/j.jmr.2004.09.021
Choi I-Y, Lee S-P, Shen J (2005b) Selective homonuclear Hartmann-Hahn transfer method for in vivo spectral editing in the human brain. Magn Reson Med 53:503–510. doi:10.1002/mrm.20381
Cocuzzo D, Lin A, Ramadan S et al (2011) Algorithms for characterizing brain metabolites in two-dimensional in vivo MR correlation spectroscopy. Conf Proc IEEE Eng Med Biol Soc 2011:4929–4934. doi:10.1109/IEMBS.2011.6091222
Cooper JR, Bloom FE, Roth RH (1970) The biochemical basis of neuropharmacology. Oxford University Press, New York
Do KQ, Trabesinger AH, Kirsten-Krüger M et al (2000) Schizophrenia: glutathione deficit in cerebrospinal fluid and prefrontal cortex in vivo. Eur J Neurosci 12:3721–3728
Dreher W, Leibfritz D (1995) On the use of 2-Dimensional-J NMR measurements for in-vivo proton MRS- measurement of homonuclear decoupled spectra without the need for short echo times. Magn Reson Med 34:331–337. doi:10.1002/mrm.1910340309
Dringen R, Gutterer JM, Hirrlinger J (2000) Glutathione metabolism in brain. Eur J Biochem 267:4912–4916. doi:10.1046/j.1432-1327.2000.01597.x
Duffy SL, Lagopoulos J, Hickie IB et al (2013) Glutathione relates to neuropsychological functioning in mild cognitive impairment. Alzheimers Dement. doi:10.1016/j.jalz.2013.01.005
Edden RAE, Barker PB (2007) Spatial effects in the detection of γ-aminobutyric acid: Improved sensitivity at high fields using inner volume saturation. Magn Reson Med 58:1276–1282
Ernst RR (1992) Nobel Lecture. Nuclear magnetic resonance Fourier transform spectroscopy. Biosci Rep 12:143–187
Ernst T, Jiang CS, Nakama H et al (2010) Lower brain glutamate is associated with cognitive deficits in HIV patients: a new mechanism for HIV-associated neurocognitive disorder. J Magn Reson Imaging: JMRI 32:1045–1053. doi:10.1002/jmri.22366
Fayed N, Modrego PJ, Rojas-Salinas G, Aguilar K (2011) Brain glutamate levels are decreased in Alzheimer's disease: a magnetic resonance spectroscopy study. Am J Alzheimers Dis Other Demen 26:450–456. doi:10.1177/1533317511421780
Frey BN, Stanley JA, Nery FG et al (2007) Abnormal cellular energy and phospholipid metabolism in the left dorsolateral prefrontal cortex of medication-free individuals with bipolar disorder: an in vivo 1H MRS study. Bipolar Disord 9(Suppl 1):119–127. doi:10.1111/j.1399-5618.2007.00454.x
Friston KJ (1997) Analyzing brain images: principles and overview. In: Frackowiak RSJ, Friston Frith CD, Dolan RJMS (eds) Human brain function. Academic, San Diego, pp 25–41
Gigante AD, Bond DJ, Lafer B et al (2012) Brain glutamate levels measured by magnetic resonance spectroscopy in patients with bipolar disorder: a meta-analysis. Bipolar Disord 14:478–487. doi:10.1111/j.1399-5618.2012.01033.x
Goddard AW, Mason GF, Almai A et al (2001) Reductions in occipital cortex GABA levels in panic disorder detected with 1 h-magnetic resonance spectroscopy. Arch Gen Psychiatry 58:556
Goddard AW, Mason GF, Appel M et al (2004) Impaired GABA neuronal response to acute benzodiazepine administration in panic disorder. Am J Psychiatry 161:2186–2193
Gonzalez-Burgos G, Hashimoto T, Lewis DA (2010) Alterations of cortical GABA neurons and network oscillations in schizophrenia. Curr Psychiatry Rep 12:335–344. doi:10.1007/s11920-010-0124-8
Goto N, Yoshimura R, Moriya J et al (2009) Reduction of brain gamma-aminobutyric acid (GABA) concentrations in early-stage schizophrenia patients: 3T Proton MRS study. Schizophr Res 112:192–193. doi:10.1016/j.schres.2009.04.026
Govindaraju V, Young K, Maudsley AA (2000) Proton NMR chemical shifts and coupling constants for brain metabolites. NMR Biomed 13:129–153

De Graaf RA, Rothman DL, Behar KL (2011) State of the art direct 13C and indirect 1H-[13C] NMR spectroscopy in vivo. A practical guide. NMR Biomed 24:958–972. doi:10.1002/nbm.1761

Graff-Radford J, Kantarci K (2013) Magnetic resonance spectroscopy in Alzheimer's disease. Neuropsychiatr Dis Treat 9:687–696. doi:10.2147/NDT.S35440

Gruber S, Frey R, Mlynárik V et al (2003) Quantification of metabolic differences in the frontal brain of depressive patients and controls obtained by 1H-MRS at 3 Tesla. Invest Radiol 38:403–408. doi:10.1097/01.rli.0000073446.43445.20

Gruetter R, Novotny EJ, Boulware SD et al (1994) Localized 13C NMR spectroscopy in the human brain of amino acid labeling from d-[1-^{13}C]glucose. J Neurochem 63:1377–1385. doi:10.1046/j.1471-4159.1994.63041377.x

Haase A, Frahm J, Matthaei D et al (1986) MR imaging using stimulated echoes (STEAM). Radiology 160:787–790

Harris K, Lin A, Bhattacharya P et al (2006) Regulation of NAA-synthesis in the human brain in vivo: Canavan's disease, Alzheimer's disease and schizophrenia. Adv Exp Med Biol 576:263–273. doi:10.1007/0-387-30172-0_18; discussion 361–3

Hasler G, Neumeister A, Van der Veen JW et al (2005) Normal prefrontal gamma-aminobutyric acid levels in remitted depressed subjects determined by proton magnetic resonance spectroscopy. Biol Psychiatry 58:969–973

Hennig J (1992) The application of phase rotation for localized in vivo proton spectroscopy with short echo times. J Magn Reson 40–49

Hermens DF, Lagopoulos J, Naismith SL et al (2012) Distinct neurometabolic profiles are evident in the anterior cingulate of young people with major psychiatric disorders. Transl Psychiatry 2:e110. doi:10.1038/tp.2012.35

Hertz L, Zielke HR (2004) Astrocytic control of glutamatergic activity: astrocytes as stars of the show. Trends Neurosci 27:735–743

Hurd R, Sailasuta N, Srinivasan R et al (2004) Measurement of brain glutamate using TE-averaged PRESS at 3T. Magn Reson Med 51:435–440

Jang DP, Lee JM, Lee E et al (2005) Interindividual reproducibility of glutamate quantification using 1.5-T proton magnetic resonance spectroscopy. Magn Reson Med 53:708–712. doi:10.1002/mrm.20387

Jarskog LF, Miyamoto S, Lieberman JA (2007) Schizophrenia: new pathological insights and therapies. Annu Rev Med 58:49–61. doi:10.1146/annurev.med.58.060904.084114

Javitt DC, Zukin SR (1991) Recent advances in the phencyclidine model of schizophrenia. Am J Psychiatry 148:1301–1308

Jeener J, Meier BH, Bachmann P, Ernst RR (1979) Investigation of exchange processes by two-dimensional NMR spectroscopy. J Chem Phys 71:4546. doi:10.1063/1.438208

Jensen JE, Frederick BD, Wang L et al (2005) Two-dimensional, J-resolved spectroscopic imaging of GABA at 4 Tesla in the human brain. Magn Reson Med 54:783–788. doi:10.1002/mrm.20644

Jones RS, Waldman AD (2004) 1H-MRS evaluation of metabolism in Alzheimer's disease and vascular dementia. Neurol Res 26:488–495. doi:10.1179/016164104225017640

Kaiser LG, Young K, Matson GB (2007) Elimination of spatial interference in PRESS-localized editing spectroscopy. Magn Reson Med 58:813–818

Kantarci K (2007) 1H magnetic resonance spectroscopy in dementia. Br J Radiol 80(Spec No 2):S146–S152. doi:10.1259/bjr/60346217

Kantarci K (2013) Proton MRS in mild cognitive impairment. J Magn Reson Imaging: JMRI 37:770–777. doi:10.1002/jmri.23800

Kantarci K, Petersen RC, Boeve BF et al (2004) 1H MR spectroscopy in common dementias. Neurology 63:1393–1398

Kantarci K, Weigand SD, Przybelski SA et al (2013) MRI and MRS predictors of mild cognitive impairment in a population-based sample. Neurology 81:126–133. doi:10.1212/WNL.0b013e31829a3329

Kato T, Takahashi S, Shioiri T et al (1994) Reduction of brain phosphocreatine in bipolar II disorder detected by phosphorus-31 magnetic resonance spectroscopy. J Affect Disord 31:125–133

Kaufman RE, Ostacher MJ, Marks EH et al (2009) Brain GABA levels in patients with bipolar disorder. Prog Neuropsychopharmacol Biol Psychiatry 33:427–434

Ke Y, Cohen BM, Bang JY et al (2000) Assessment of GABA concentration in human brain using two-dimensional proton magnetic resonance spectroscopy. Psychiatry Res 100:169–178

Kegeles LS, Humaran TJ, Mann JJ (1998) In vivo neurochemistry of the brain in schizophrenia as revealed by magnetic resonance spectroscopy. Biol Psychiatry 44:382–398

Keltner JR, Wald LL, Frederick BD, Renshaw PF (1997) In vivo detection of GABA in human brain using a localized double-quantum filter technique. Magn Reson Med 37:366–371

Kraguljac NV, Reid M, White D et al (2012) Neurometabolites in schizophrenia and bipolar disorder - a systematic review and meta-analysis. Psychiatry Res 203:111–125. doi:10.1016/j.pscychresns.2012.02.003

Kreis R, Ernst T, Ross BD (1993) Absolute quantitation of water and metabolites in the human brain. II. Metabolite concentrations. J Magn Reson - Ser B 102:9–19. doi:10.1006/jmrb.1993.1056

Lagopoulos J, Hermens DF, Tobias-Webb J et al (2013) In vivo glutathione levels in young persons with bipolar disorder: A magnetic resonance spectroscopy study. J Psychiatr Res 47:412–417. doi:10.1016/j.jpsychires.2012.12.006

Lauterbur PC (1989) Image formation by induced local interactions. Examples employing nuclear magnetic resonance. 1973. Clin Orthop Relat Res (244): 3–6

Lin A, Ross BD, Harris K, Wong W (2005) Efficacy of proton magnetic resonance spectroscopy in neurological diagnosis and neurotherapeutic decision making. NeuroRx 2:197–214. doi:10.1602/neurorx.2.2.197

Lin AP, Shic F, Enriquez C, Ross BD (2003) Reduced glutamate neurotransmission in patients with Alzheimer's disease–an in vivo 13C magnetic resonance spectroscopy study. Magn Reson Mater Phys, Biol Med 16:29–42

Long Z, Medlock C, Dzemidzic M et al (2013) Decreased GABA levels in anterior cingulate cortex/medial prefrontal cortex in panic disorder. Prog Neuropsychopharmacol Biol Psychiatry 44:131–135. doi:10.1016/j.pnpbp.2013.01.020

Luykx JJ, Laban KG, Van den Heuvel MP et al (2012) Region and state specific glutamate downregulation in major depressive disorder: a meta-analysis of (1) H-MRS findings. Neurosci Biobehav Rev 36:198–205. doi:10.1016/j.neubiorev.2011.05.014

Lymer K, Haga K, Marshall I et al (2007) Reproducibility of GABA measurements using 2D J-resolved magnetic resonance spectroscopy. Magn Reson Imaging 25:634–640. doi:10.1016/j.mri.2006.10.010

Maddock RJ, Buonocore MH (2012) MR spectroscopic studies of the brain in psychiatric disorders. Curr Top Behav Neurosci. doi:10.1007/7854_2011_197

Mandal PK, Tripathi M, Sugunan S (2012) Brain oxidative stress: detection and mapping of anti-oxidant marker "Glutathione" in different brain regions of healthy male/female, MCI and Alzheimer patients using non-invasive magnetic resonance spectroscopy. Biochem Biophys Res Commun 417:43–48. doi:10.1016/j.bbrc.2011.11.047

Marsman A, Van den Heuvel MP, Klomp DWJ et al (2013) Glutamate in schizophrenia: a focused review and meta-analysis of ^{1}H-MRS studies. Schizophr Bull 39:120–129. doi:10.1093/schbul/sbr069

Mason GF, Gruetter R, Rothman DL et al (1995) Simultaneous determination of the rates of the TCA cycle, glucose utilization, μ-ketoglutarate/Glutamate exchange, and glutamine synthesis in human brain by NMR. J Cereb Blood Flow Metab 15:12–25

Matsuzawa D, Hashimoto K (2011) Magnetic resonance spectroscopy study of the antioxidant defense system in schizophrenia. Antioxid Redox Signal 15:2057–2065. doi:10.1089/ars.2010.3453

Matsuzawa D, Obata T, Shirayama Y et al (2008) Negative correlation between brain glutathione level and negative symptoms in schizophrenia: a 3T 1H-MRS study. PloS one 3:e1944. doi:10.1371/journal.pone.0001944

Maudsley AA, Hilal SK, Perman WH, Simon HE (1983) Spatially resolved high resolution spectroscopy by "Four-Dimensional" NMR. J Magn Reson 147–152

McLean MA, Busza AL, Wald LL et al (2002) In vivo GABA+ measurement at 1.5T using a PRESS-localized double quantum filter. Magn Reson Med 48:233–241

Minoshima S, Giordani B, Berent S et al (1997) Metabolic reduction in the posterior cingulate cortex in very early Alzheimer's disease. Ann Neurol 42:85–94. doi:10.1002/ana.410420114

Moffett JR, Namboodiri MA, Neale JH (1993) Enhanced carbodiimide fixation for immunohistochemistry: application to the comparative distributions of N-acetylaspartylglutamate and N-acetylaspartate immunoreactivities in rat brain. J Histochem Cytochem 41:559–570

Moffett JR, Ross B, Arun P et al (2007) N-Acetylaspartate in the CNS: from neurodiagnostics to neurobiology. Prog Neurobiol 81:89–131. doi:10.1016/j.pneurobio.2006.12.003

Mosley RL, Benner EJ, Kadiu I et al (2006) Neuroinflammation, oxidative stress and the pathogenesis of Parkinson's disease. Clin Neurosci Res 6:261–281. doi:10.1016/j.cnr.2006.09.006

Mullins PG, Chen H, Xu J et al (2008) Comparative reliability of proton spectroscopy techniques designed to improve detection of J-coupled metabolites. Magn Reson Med 60:964–969. doi:10.1002/mrm.21696

Olman CA, Davachi L, Inati S (2009) Distortion and signal loss in medial temporal lobe. PloS one 4:e8160. doi:10.1371/journal.pone.0008160

Olsen RW, DeLorey TM (1999) GABA synthesis, uptake and release. In: Siegel GJ, Agranoff BW, Albers RW, Fisher SK, Uhler MD (eds) Basic neurochemistry: molecular, cellular and medical aspects. Lippincott-Raven, Philadelphia

Ongür D, Prescot AP, Jensen JE et al (2009) Creatine abnormalities in schizophrenia and bipolar disorder. Psychiatry Res 172:44–48. doi:10.1016/j.pscychresns.2008.06.002

Ongür D, Prescot AP, McCarthy J et al (2010) Elevated gamma-aminobutyric acid levels in chronic schizophrenia. Biol Psychiatry 68:667–670. doi:10.1016/j.biopsych.2010.05.016

Öz G, Terpstra M, Tkáč I et al (2006) Proton MRS of the unilateral substantia nigra in the human brain at 4 tesla: detection of high GABA concentrations. Magn Reson Med 55:296–301

Pellerin L, Magistretti P (1994) Glutamate uptake into astrocytes stimulates aerobic glycolysis: A mechanism coupling neuronal activity to glucose utilization. Proc Natl Acad Sci U S A 91:10625–10629

Penner J, Rupsingh R, Smith M et al (2010) Increased glutamate in the hippocampus after galantamine treatment for Alzheimer disease. Prog Neuropsychopharmacol Biol Psychiatry 34:104–110. doi:10.1016/j.pnpbp.2009.10.007

Phan KL, Fitzgerald DA, Cortese BM et al (2005) Anterior cingulate neurochemistry in social anxiety disorder: 1H-MRS at 4 Tesla. Neuroreport 16:183–186

Pollack MH, Jensen JE, Simon NM et al (2008) High-field MRS study of GABA, glutamate and glutamine in social anxiety disorder: response to treatment with levetiracetam. Prog Neuropsychopharmacol Biol Psychiatry 32:739–743

Port JD, Agarwal N (2011) MR spectroscopy in schizophrenia. J Magn Reson Imaging: JMRI 34:1251–1261. doi:10.1002/jmri.22787

Posner MJ, Raichle ME (1997) Images of mind. WH Freeman, New York

Posse S, Otazo R, Dager SR, Alger J (2013) MR spectroscopic imaging: principles and recent advances. J Magn Reson Imaging 37:1301–1325. doi:10.1002/jmri.23945

Provencher SW (2001) Automatic quantitation of localized in vivo 1H spectra with LCModel. NMR Biomed 14:260–264

Provencher SW (1993) Estimation of metabolite concentrations from localized in vivo proton NMR spectra. Magn Reson Med 30:672–679

Ramadan S (2007) Phase-rotation in in-vivo localised spectroscopy. Concepts Magn Reson 30:147–153

Ramadan S, Andronesi OC, Stanwell P et al (2011) Use of in vivo two-dimensional MR spectroscopy to compare the biochemistry of the human brain to that of glioblastoma. Radiology 259:540–549. doi:10.1148/radiol.11101123

Rezin GT, Amboni G, Zugno AI et al (2009) Mitochondrial dysfunction and psychiatric disorders. Neurochem Res 34:1021–1029. doi:10.1007/s11064-008-9865-8

Rigotti DJ, Inglese M, Gonen O (2007) Whole-brain N-acetylaspartate as a surrogate marker of neuronal damage in diffuse neurologic disorders. AJNR Am J Neuroradiol 28:1843–1849. doi:10.3174/ajnr.A0774

Rinck P (2012) Magnetic resonance in medicine. The Basic Textbook of the European Magnetic Resonance Forum. 6th edn. Electronic version 6.1. Available at www.magnetic-resonance.org.

Rosen Y, Lenkinski RE (2007) Recent advances in magnetic resonance neurospectroscopy. Neurotherapeutics 4:330–345. doi:10.1016/j.nurt.2007.04.009

Ross B, Bluml S (2001) Magnetic resonance spectroscopy of the human brain. Anat Rec 265:54–84

Ross B, Lin A, Harris K et al (2003) Clinical experience with 13C MRS in vivo. NMR Biomed 16:358–369

Ross BD (2000) Real or imaginary? Human metabolism through nuclear magnetism. IUBMB Life 50:177–187. doi:10.1080/152165400300001499

Ross BD, Bluml S, Cowan R et al (1997) In vivo magnetic resonance spectroscopy of human brain: the biophysical basis of dementia. Biophys Chem 68:161–172

Rowland LM, Kontson K, West J et al (2012) In vivo measurements of glutamate, GABA, and NAAG in schizophrenia. Schizophr Bull. doi:10.1093/schbul/sbs092

Sailasuta N, Harris K, Tran T, Ross B (2011) Minimally invasive biomarker confirms glial activation present in Alzheimer's disease: a preliminary study. Neuropsychiatr Dis Treat 7:495–499

Sanacora G, Treccani G, Popoli M (2012) Towards a glutamate hypothesis of depression: an emerging frontier of neuropsychopharmacology for mood disorders. Neuropharmacology 62:63–77. doi:10.1016/j.neuropharm.2011.07.036

Satoh T, Yoshioka Y (2006) Contribution of reduced and oxidized glutathione to signals detected by magnetic resonance spectroscopy as indicators of local brain redox state. Neurosci Res 55:34–39. doi:10.1016/j.neures.2006.01.002

Schousboe A (2003) Role of astrocytes in the maintenance and modulation of glutamatergic and GABAergic neurotransmission. Neurochem Res 28:347–352. doi:10.1023/a:1022397704922

Schousboe A, Waagepetersen H (2005) Role of astrocytes in glutamate homeostasis: Implications for excitotoxicity. Neurotox Res 8:221–225. doi:10.1007/bf03033975

Schubert F, Gallinat J, Seifert F, Rinneberg H (2004) Glutamate concentrations in human brain using single voxel proton magnetic resonance spectroscopy at 3 Tesla. Neuroimage 21:1762–1771

Schulte RF, Boesiger P (2006) ProFit: two-dimensional prior-knowledge fitting of J-resolved spectra. NMR Biomed 19:255–263. doi:10.1002/nbm.1026

Schulte RF, Lange T, Beck J et al (2006) Improved two-dimensional J-resolved spectroscopy. NMR Biomed 19:264–270. doi:10.1002/nbm.1027

Shonk TK, Moats RA, Gifford P et al (1995) Probable Alzheimer disease: diagnosis with proton MR spectroscopy. Radiology 195:65–72

Sibson NR, Dhankhar A, Mason GF et al (1998) Stoichiometric coupling of brain glucose metabolism and glutamatergic neuronal activity. Proc Natl Acad Sci U S A 95:316–321

Simister RJ, McLean MA, Barker GJ, Duncan JS (2003) A proton magnetic resonance spectroscopy study of metabolites in the occipital lobes in epilepsy. Epilepsia 44:550–558

Starcuk Z, Starcuk Z Jr, Horky J (2001) "Baseline" problems in very short echo-time proton MR spectroscopy of low molecular weight metabolites in the brain. Meas Sci Rev 1:17–20

Strawn JR, Chu W-J, Whitsel RM et al (2013) A pilot study of anterior cingulate cortex neurochemistry in adolescents with generalized anxiety disorder. Neuropsychobiology 67:224–229. doi:10.1159/000347090

Tayoshi S, Nakataki M, Sumitani S et al (2010) GABA concentration in schizophrenia patients and the effects of antipsychotic medication: a proton magnetic resonance spectroscopy study. Schizophr Res 117:83–91. doi:10.1016/j.schres.2009.11.011

Terpstra M, Ugurbil K, Gruetter R (2002) Direct in vivo measurement of human cerebral GABA concentration using MEGA-editing at 7 Tesla. Magn Reson Med 47:1009–1012

Terpstra M, Vaughan TJ, Ugurbil K et al (2005) Validation of glutathione quantitation from STEAM spectra against edited 1H NMR spectroscopy at 4 T: application to schizophrenia. Magma (New York, NY) 18:276–282. doi:10.1007/s10334-005-0012-0

Thomas MA, Yue K, Binesh N et al (2001) Localized two-dimensional shift correlated MR spectroscopy of human brain. Magn Reson Med 46:58–67

Urenjak J, Williams SR, Gadian DG, Noble M (1992) Specific expression of N-acetylaspartate in neurons, oligodendrocyte-type-2 astrocyte progenitors, and immature oligodendrocytes in vitro. J Neurochem 59:55–61

Vanhamme L, Van den Boogaart A, Van Huffel S (1997) Improved method for accurate and efficient quantification of MRS data with use of prior knowledge. J Magn Reson 129:35–43. doi:10.1006/jmre.1997.1244

Waddell KW, Avison MJ, Joers JM, Gore JC (2007) A practical guide to robust detection of GABA in human

brain by J-difference spectroscopy at 3 T using a standard volume coil. Magn Reson Imaging 25:1032–1038. doi:10.1016/j.mri.2006.11.026

Wijtenburg SA, Knight-Scott J (2011) Very short echo time improves the precision of glutamate detection at 3T in 1H magnetic resonance spectroscopy. J Magn Reson Imaging 34:645–652

Wood SJ, Berger GE, Wellard RM et al (2009) Medial temporal lobe glutathione concentration in first episode psychosis: a 1H-MRS investigation. Neurobiol Dis 33:354–357. doi:10.1016/j.nbd.2008.11.018

Yang S, Hu J, Kou Z, Yang Y (2008) Spectral simplification for resolved glutamate and glutamine measurement using a standard STEAM sequence with optimized timing parameters at 3, 4, 4.7, 7, and 9.4 T. Magn Reson Med// 59:236–244. doi:10.1002/mrm.21463

Yoon JH, Maddock RJ, Rokem A et al (2010) GABA concentration is reduced in visual cortex in schizophrenia and correlates with orientation-specific surround suppression. J Neurosci 30:3777–3781

Zhou J, van Zijl PCM (2006) Chemical exchange saturation transfer imaging and spectroscopy. Prog Nucl Magn Reson Spectrosc 48:109–136. doi:10.1016/j.pnmrs.2006.01.001

Zwanzger P, Zavorotnyy M, Gencheva E et al (2013) Acute shift in glutamate concentrations following experimentally induced panic with cholecystokinin tetrapeptide-A 3T-MRS study in healthy subjects. Neuropsychopharmacology 38:1648–1654. doi:10.1038/npp.2013.61